Published in final edited form as:
Meteorit Planet Sci. 2015 July 16; 50(7): 1197–1216. doi:10.1111/maps.12461.

Pb-Pb dating of individual chondrules from the CB_a chondrite Gujba: Assessment of the impact plume formation model

Jean Bollard[*], **James N. Connelly**, and **Martin Bizzarro**
Centre for Star and Planet Formation, Natural History Museum of Denmark, DK-1350 Copenhagen, Denmark

Abstract

The CB chondrites are metal-rich meteorites with characteristics that sharply distinguish them from other chondrite groups. Their unusual chemical and petrologic features and a young formation age of bulk chondrules dated from the CB_a chondrite Gujba are interpreted to reflect a single-stage impact origin. Here, we report high-precision internal isochrons for four individual chondrules of the Gujba chondrite to probe the formation history of CB chondrites and evaluate the concordancy of relevant short-lived radionuclide chronometers. All four chondrules define a brief formation interval with a weighted mean age of 4562.49 ± 0.21 Myr, consistent with its origin from the vapor-melt impact plume generated by colliding planetesimals. Formation in a debris disk mostly devoid of nebular gas and dust sets an upper limit for the solar protoplanetary disk lifetime at 4.8 ± 0.3 Myr. Finally, given the well-behaved Pb-Pb systematics of all four chondrules, a precise formation age and the concordancy of the Mn-Cr, Hf-W, and I-Xe short-lived radionuclide relative chronometers, we propose that Gujba may serve as a suitable time anchor for these systems.

Introduction

Chondrules are mm- to cm-sized, igneous silicate spherules that occur in abundance (up to 80 wt%) in chondrite meteorites. They have been extensively studied (Grossman et al. 1988; Jones et al. 2000, 2005; Connolly and Desch 2004; Hewins et al. 2005; Rubin 2005, 2010; Connolly et al. 2006; Lauretta et al. 2006) and comprise ferromagnesian silicates olivine, pyroxene, metal (Fe, Ni), and glassy or microcrystalline mesostasis. Chondrules formed as molten droplets during transient heating events followed by rapid cooling and crystallization result in a variety of textures from porphyritic to barred/skeletal, radial, and cryptocrystalline (Gooding and Keil 1981; Hewins 1997; Connolly and Love 1998; Krot et al. 2009), which reflect varying thermal histories. Typical peak temperatures and cooling rates are 1750–2100 K and 10–1000 Kh^{-1} (Desch et al. 2012). Recent isotope data (Connelly et al. 2012) indicate that chondrule formation in the accretion disk (hereafter referred to as “nebular chondrules”) started contemporaneously with CAI formation and lasted at least 2.5 Myr.

[*]Corresponding author. jean.bollard@snm.ku.dk.
Editorial Handling—Dr. A. J. Timothy Jull

Europe PMC Funders Author Manuscripts

Chondrules reflect some of the most energetic processes that operated in the early solar system. The source of the thermal energy is still vigorously debated with different models including shock waves (Boss and Graham 1993; Connolly and Love 1998; Hood 1998), current sheets (Joung et al. 2004), colliding molten planetesimals (Sanders and Taylor 2005; Asphaug et al. 2011), X-winds (Shu et al. 1997), and magnetized disk winds (Salmeron and Ireland 2012). Nebular shock waves currently represents the most widely accepted model (Desch et al. 2012) with triggering mechanisms including X-ray flares (Nakamoto et al. 2005), accretion shocks (Ruzmaikina and Ip 1994; Nelson and Ruffert 2005), and planetesimal bow shocks (Ciesla et al. 2004; Hood et al. 2005, 2009), and those driven by gravitational instabilities in the disk (Boss and Durisen 2005; Boley and Durisen 2008). All these models take place in the presence of gas in the solar nebula. However, some models (Urey and Craig 1953; Urey 1967; Sanders 1996; Sanders and Taylor 2005; Asphaug et al. 2011) ascribe chondrule formation to a planetary setting, involving collisions between planetary bodies once the gas in the disk has mostly dissipated. The discovery of the CB-CH chondrites and their unique properties brought the first serious arguments in favor of chondrule formation in a planetary setting (Krot et al. 2005). More recently, Johnson et al. (2015) successfully simulated impact-produced chondrules, with formation starting 10^3–10^4 years after T_0 and lasting more than 5 Myr. This opens the possibility for a more universal and global chondrule formation scenario.

This paper reports precise internal isochrons of four individual chondrules from the CB Gujba chondrite. These new Pb-Pb ages for single Gujba chondrules are useful for two reasons. First, they provide a test of the impact model for the Gujba chondrite, which predicts a rapid formation. Second, if a single formation age is verified, Gujba, with its diversity of inclusions, may serve as a useful anchor to map relative chronometers based on short-lived radionuclides with appropriate half-lives onto an absolute time scale. This second point reflects the brief formation interval and rapid cooling of both metal and silicate material predicted by an impact formation scenario such that all chronometric systems would have closed simultaneously.

CB Chondrite Characteristics

The CB chondrites (Bencubbin-like) group consists of six meteorites, Bencubbin, Gujba, Weatherford, Mac Alpine Hills 02675 (MAC), Hammadah al Hamra 237 (HaH237), and Queen Alexandra Range (QUE 94411), which are characterized by high (60–70 vol%) abundance of Fe-Ni metal ± sulfide, depletion in both volatile and moderately volatile elements, rare refractory inclusions, and near absence of fine-grained matrix (Campbell et al. 2002; Krot et al. 2002; Rubin et al. 2003). These meteorites are subdivided into CB_a (Bencubbin, Gujba, and Weatherford) and CB_b (MAC, HaH237, and QUE 94411) types. The CB_b group are finer grained than the CB_a group, contain rare uniformly ^{16}O poor refractory inclusions, and abundant chemically zoned Fe-Ni metal grains that are not present in CB_a. On the other hand, the CB_a group exhibits large (~cm sized) silicate chondrules and unzoned metal nodules. Metal in CB_a chondrites is kamacite, with nickel contents varying between 4.8 and 8.2 wt%. Metal also contains sulfide inclusions (Rubin et al. 2003). All CB silicate chondrules are metal free and lack fine-grained matrix-like rims, suggesting formation in a dust-poor or dust-free environment. The chondrules lack relict grains and

coarse-grained igneous rims, indicative of multiple melting events commonly recorded by nebular chondrules (Rubin 2000). CB chondrules also have exclusively nonporphyritic textures, indicating that the precursor material was almost fully molten, nearly free of nuclei, and then rapidly cooled (Krot et al. 2001, 2005). The observed depletion in moderately volatile elements in chondrules and metal requires their formation at high ambient temperature, above the highest condensation temperature (1200 K) of Mn, Na, K, S, Cu, Zn, and Ga. Recently, Fedkin et al. (2013) observed that Pd/Ir ratios in unzoned metal grains in CB_a chondrites require condensation from a gas with partial pressures of siderophiles many orders of magnitude higher than is considered possible for the solar nebula. Olsen et al. (2013) observed a nonfractionated, mass-independent ^{26}Mg composition in Gujba chondrules, indicating a late-stage formation from an initially homogeneous magnesium reservoir.

The skeletal/barred nonporphyritic textures of chondrules in the CB chondrites cannot be duplicated by monotonous linear cooling, as is the case for nebular porphyritic chondrules, but require a complex heating and cooling history consistent with a vapor plume (Condie 2012). An impact would produce a range of pressures and temperatures that would change as the impact plume evolved. The different silicate and metal grains that occur in both the CB_a and the CB_b chondrites formed as a result of the impact but at different stages or locations in the vapor plume. From simulation, Fedkin et al. (2014) found that the formation of CB chondrites in an impact plume would require that the two impactors had contrasting silicate compositions with relative proportions varying spatially within the plume, in agreement with the model above.

Finally, based on the characteristic features described above, and one multichondrule age for Gujba of 4562.68 ± 0.49 Myr (all uncertainties in this paper are at 95% confidence level), Krot et al. (2005) suggested that CB components (chondrules and metal grains) formed in a single-stage energetic event consistent with a vapor-melt plume produced by a giant hypersonic impact between planetary embryos.

Gujba Formation Age—We review below the available age data for Gujba based on various chronometers, summarized in Table 1.

^{207}Pb-^{206}Pb Dating: The first attempt to date the CB_a Gujba chondrites was reported by Krot et al. (2005) where they applied the absolute Pb-Pb dating method on silicate chondrules. They picked compositionally distinct fractions from three chondrules that were combined and regressed to define an average Pb isotopic composition of all fractions. They obtained an absolute age of 4562.68 ± 0.49 Myr, which represents the youngest chondrule age from any chondrite. To calculate this age, they used the $^{238}U/^{235}U$ ratio of 137.88, traditionally assumed to represent the natural uranium isotopic composition of the solar system. However, Brennecka et al. (2010) demonstrated that the uranium composition is nonhomogeneous in some meteoritic materials. Connelly et al. (2012) defined a new present-day $^{238}U/^{235}U$ ratio of 137.786 ± 0.013 for inner solar system objects other than calcium-aluminum inclusions (CAIs), which requires a −1 Myr age adjustment to all existing ages that were based on $^{238}U/^{235}U$ ratio of 137.88. To be noted that Connelly et al. (2012) also reported a bulk uranium isotopic composition for the Gujba chondrite of 137.794

± 0.014, consistent with their average value of 137.786 ± 0.013. The majority of U in Gujba is host by the chondrules; therefore, the bulk value is assumed to be representative of the chondrules' composition. However, it is indistinguishable within uncertainty from the precise estimate of 137.786 ± 0.013 for inner solar system objects, which is then the value retained for Gujba chondrules' absolute Pb-Pb dating. The uncertainty of the $^{238}U/^{235}U$ value contributes an error of ±0.14 Myr to Pb-Pb ages at ca. 4.5 Gyr, which is propagated together with the isochron Pb-Pb age errors in quadrature. Using this new uranium isotopic composition, the absolute Pb-Pb age of Gujba chondrules dated by Krot et al. (2005) is recalculated as 4561.68 ± 0.51 Myr.

We note that a $^{238}U/^{235}U$ value of 137.794 ± 0.027 was recently proposed by Goldmann et al. (2015) as representing the bulk composition of the solar system. This estimate, which is identical to the value proposed by Connelly et al. (2012) albeit with a larger uncertainty, is based on terrestrial and meteorite samples, including objects that define $^{238}U/^{235}U$ variability. However, when scrutinizing the data set of Goldmann et al. (2015), serious flaws become apparent. The reported $^{238}U/^{235}U$ variability, mostly expressed in ordinary chondrites of high metamorphic grade, is positively correlated with the U content. This behavior is expected if the $^{238}U/^{235}U$ variability reflects stable U isotope fractionation associated with the mobilization of phosphates during thermal metamorphism. We note that the size of the samples characterized by $^{238}U/^{235}U$ variability were typically small (500–600 mg), which makes these measurements highly susceptible to the heterogeneous distribution of phosphates. Indeed, much larger samples (>5 g) of high metamorphic grade ordinary chondrites measured in the same study did not show $^{238}U/^{235}U$ variability. Thus, we conclude that the bulk of the $^{238}U/^{235}U$ variability reported by Goldmann et al. (2015) is secondary and due to unrepresentative sampling of the chondrites. In contrast, the solar $^{238}U/^{235}U$ value determined by Connelly et al. (2012) is based on large sample aliquots (>3 g) of pristine and unmetamorphed carbonaceous and ordinary chondrites and, thus, we infer that their estimate remains the most robust determination of the solar $^{238}U/^{235}U$ value.

^{53}Mn-^{53}Cr Chronometer: The manganese-chromium short-lived radionuclide chronometer exploits the decay of ^{53}Mn to ^{53}Cr with a half-life of 3.7 ± 0.2 Myr (Holden 1990). Recent available data support a uniform distribution of the ^{53}Mn nuclide in the early solar system (Yamashita et al. 2010) supporting the use of the ^{53}Mn-^{53}Cr system to probe the early solar system chronometry. Yamashita et al. (2010) analyzed the Cr isotopic composition of different Gujba chondrules and metal grains. The $\varepsilon^{53}Cr$ values of both chondrules and metal display a strong correlation with the $^{55}Mn/^{52}Cr$ ratio, which they interpret to represent an isochron with a slope defining an initial $^{53}Mn/^{55}Mn$ ratio of $(3.18 \pm 0.52) \times 10^{-6}$. The two most commonly used time anchors for this chronometer are angrites D'Orbigny and LEW 86010, with U-corrected absolute Pb ages and initial $^{53}Mn/^{55}Mn$ ratios of 4563.37 ± 0.25 Myr and $(3.24 \pm 0.04) \times 10^{-6}$, and 4557.53 ± 0.25 Myr and $(1.25 \pm 0.07) \times 10^{-6}$, respectively (Lugmair and Galer 1992; Glavin et al. 2004; Amelin 2008; Brennecka and Wadhwa 2012). Using these two time anchors, the Mn-Cr age of Gujba chondrules/metal grain corresponds to 4563.3 ± 1.0 Myr and 4562.5 ± 1.2 Myr. Yamashita et al. (2010) interpreted the $\varepsilon^{53}Cr$ data and the indistinguishable $\varepsilon^{54}Cr$ values for both chondrules and

metal grain to be consistent with the formation of Gujba chondrules and metal from a common, isotopically uniform reservoir.

^{182}Hf-^{182}W Chronometer: The hafnium-tungsten short-lived radionuclide chronometer is based on the decay of ^{182}Hf to ^{182}W with a half-life of 8.90 ± 0.09 Myr (Vockenhuber et al. 2004). Currently available data support the proposal that the ^{182}Hf nuclide was uniformly distributed in the early solar system with an initial ^{182}Hf/^{180}Hf ratio of (9.85 ± 0.40) × 10^{-5} and initial ε^{182}W of −3.49 ± 0.07 (Kleine et al. 2005; Holst et al. 2013; Kruijer et al. 2014b). Because Hf is lithophile and W is siderophile, fractionation of Hf from W occurs during metal-silicate separation. Thus, the ^{182}Hf-^{182}W system is well-suited to date the segregation of liquid Fe-Ni metal from silicates. It is one of the most widely used chronometers to constrain the timing of core formation in asteroids in the early solar system. Kleine et al. (2005) analyzed different metal fractions from Gujba and two other CB chondrites, HaH237 and Bencubbin. Their initial ε^{182}W value is more radiogenic than that of CAIs and magmatic iron meteorites examined in the same study. The CB chondrites all exhibit indistinguishable initial ε^{182}W values with a weighted average of −2.97 ± 0.16. From the initial ε^{182}W value, a model age can be calculated using a time anchor and comparing the two ε^{182}W values to the present-day ε^{182}W value of chondrites, assuming that both objects formed from a reservoir having chondritic ratios of refractory elements. Assuming a batch equilibration model between the two impactors with chondritic W isotope composition and Hf/W elemental compositions, a chondritic ε^{182}W value of −1.9 ± 0.1 (Kleine et al. 2004), and using the CAIs as a time anchor with an initial ε^{182}W value of −3.49 ± 0.07 (Connelly et al. 2012; Kruijer et al. 2014b), the W isotopic composition of Gujba metal corresponds to an absolute age of 4562.2 ± 2.4 Myr. This postdates by at least 3 Myr core formation in the parent asteroids of magmatic iron meteorites (Kruijer et al. 2013, 2014a), consistent with late formation from volatilized and recondensed metal-rich material during a high-energy planetary impact in a gas-free disk.

^{129}I-^{129}Xe Chronometer: The iodine-xenon short-lived radionuclide chronometer, which was recently reviewed by Gilmour et al. (2006), is based on the decay of ^{129}I–^{129}Xe, with a half-life of 17 ± 1 Myr (Holden 1990). The uniformity of the initial iodine ratio, ^{129}I/^{127}I, and its application as a chronometer, is supported by the correspondence of isochron ages with those provided by other radioisotope dating systems (Brazzle et al. 1999; Gilmour et al. 2006, 2009). Two recent studies (Gilmour et al. 2009; Pravdivtseva et al. 2014) have investigated the iodine isotopic composition in Gujba chondrules. They reported a very low concentration of radiogenic ^{129}Xe in eight chondrules, and high concentration in one chondrule, and the latter produced a precise I-Xe isochron with an initial ^{129}I/^{127}I of (1.16 ± 0.02) × 10^{-4}. Despite the lack of an absolute Pb-Pb age, the Shallowater aubrite is the most widely used reference standard and, therefore, time anchor for the I-Xe system with an initial ^{129}I/^{127}I of 1.072 × 10^{-4} (Brazzle et al. 1999). An absolute age for Shallowater is based on an interpolation between I-Xe isochrons and the Pb-Pb ages of a suite of meteorites and inclusions to define an estimated absolute age of 4562.3 ± 0.8 Myr for Shallowater (Gilmour et al. 2009). Using a U-corrected age of 4561.3 ± 0.8 Myr for Shallowater, I-Xe isochron for the one Gujba chondrule corresponds to an absolute age of 4563.2 ± 1.3 Myr.

^{26}Al-^{26}Mg Chronometer: The aluminum-magnesium short-lived radionuclide chronometer is based on the decay of ^{26}Al to ^{26}Mg with a half-life of 0.73 Myr. The Pb-Pb age of Gujba chondrules corresponds to 7 half-lives of ^{26}Al such that most of the ^{26}Al had already decayed by the time the chondrules formed. This is confirmed by Olsen et al. (2013) who reported no resolvable ^{26}Mg excess in Gujba chondrules.

Methods

Samples and Sampling Procedure

Two adjacent slabs, with dimensions of 7 cm in diameter and 4.5 mm thick, were used in this study. They consist of three major components (1) metal nodules, (2) chondrules, and (3) interchondrule brecciated material. The majority of chondrules occur on both slabs. The largest chondrules from the slab containing the greatest mass of each inclusion was extracted and analyzed. The complementary piece was polished and imaged with a Philips SL-40 scanning electron microscope (SEM) with backscattered electron beam (BSE) at the Geological Institute at the University of Copenhagen. The chondrules were mapped in Mg, Ca, and Al with an energy dispersive X-ray detector.

The chondrules were extracted using a 250 μm diamond-coated pendulum wire saw. The remaining surrounding material was removed with a variable speed hand Dremmel® fitted with cone-shaped diamond-coated drilling tool. Each chondrule was coarsely crushed in an agate mortar and approximately 100 mg was sampled for each chondrule.

The Pb-Pb Chronometer

The Pb-Pb chronometer relies on two isotopes of U, ^{238}U and ^{235}U, that decay in a chain to stable Pb isotopes, ^{206}Pb and ^{207}Pb, respectively, resulting in $^{207}Pb_r/^{206}Pb_r$ (where r denotes radiogenic) ratios that correspond to the amount of time passed since the system closed, by the equation:

$$\frac{^{207}\mathrm{Pb_r}}{^{206}\mathrm{Pb_r}} = \left(\frac{^{235}\mathrm{U}}{^{238}\mathrm{U}}\right)\left(\frac{\left(e^{\lambda_{235}t}-1\right)}{\left(e^{\lambda_{238}t}-1\right)}\right)$$

where λ_{235} and λ_{238} are the decay constants for ^{235}U and ^{238}U, respectively, and t = time. The $^{235}U/^{238}U$ ratio has been defined as invariant for solids in the inner solar system (except CAIs) with a value of 1/(137.786 ± 0.013) (Connelly et al. 2012). Thus, the calculation of an age requires the precise determination of the $^{207}Pb/^{206}Pb$ ratio of the radiogenic Pb (Pb_r). However, samples with pure radiogenic component are rare. Most samples contain one or more additional components including: initial Pb (Pb_i), which was incorporated into the sample during its formation and/or contaminant Pb (Pb_c), which may comprise a number of different subcomponents with similar isotopic compositions, including a ubiquitous laboratory blank. As such, the $^{207}Pb/^{206}Pb$ ratio of Pb_r is most commonly calculated by extrapolating from an array of measured Pb isotopic values that represent varying mixtures of radiogenic Pb with a second component, which can be either Pb_i or a single Pb_c. In the absence of contamination, most natural systems represent a binary mixture between Pb_i and

Pb_r. Therefore, a thorough cleaning procedure of the samples is required prior to progressive dissolution to reduce or eliminate terrestrial contamination.

Cleaning and Stepwise Dissolution Routine

All samples were first rinsed 10 times in distilled water and transferred to a 7 ml Savillex® vial. They were first washed in five cycles of alternating distilled ethanol, acetone, and water that included 15 min on hot plate (110 °C) and 5 min of ultrasonication. This was followed by six steps of 0.01 M HBr that included 90 min on hotplate (110 °C) and 5 min of ultrasonication. During the entire procedure, the same Eppendorf® pipette tip was used to transfer regents from the Savillex® vial. The samples were progressively digested according to the stepwise dissolution method developed by Connelly and Bizzarro (2009). This procedure uses different acids of progressively higher strength to parse radiogenic lead (Pb_r) into aliquots with a range of $^{204}Pb/^{206}Pb$ ratios to obtain a well-constrained regression and intercept in $^{204}Pb/^{206}Pb$ versus $^{207}Pb/^{206}Pb$ space. For each sample, a total of 11–13 dissolution steps were used, starting with dilute HBr and then alternating between HCl and HNO_3 with increasing concentration (see Table 5). From the eighth step onwards, HF is used from 1M to full strength 28M. The first use of HF typically releases the most radiogenic Pb by attacking the pyroxene phases, which we assume to be the main host of uranium (Amelin et al. 2005). The fractions were then dried down and redissolved in 7M HNO_3. Once fully in solution, an equal atom ^{202}Pb-^{205}Pb tracer was added to allow for internally corrected mass fractionation during analyses by thermal ionization mass spectrometry. The mixture is dried down again and redissolved in 1M HBr, the appropriate acid for the first chemical separation step. Pb is finally separated from matrix elements and purified with a two-pass HBr-HNO_3 chemistry with 0.055 ml anion columns after Connelly and Bizzarro (2009).

Metal Nodule—A single metal nodule was also extracted from the same slab of Gujba in an attempt to constrain the Pb isotopic composition of the initial Pb for this meteorite. The metal was cleaned in four cycles of alternating distilled ethanol, acetone, and water that included 15 min on hot plate (110 °C) and 5 min of ultrasonication. The final cleaning step included 48 h on a hot plate (110 °C) in water. Six digestion steps used acids ranging from 0.01M HBr to 6M HCl.

Lead Isotope Measurements

The purified Pb was analyzed on a Thermo-Fisher Triton thermal ionization mass spectrometer at the Centre for Star and Planet Formation (Natural History Museum of Denmark—University of Copenhagen). It is equipped with nine Faraday detectors and one axial secondary electron multiplier–ion counting (SEM–IC) system. Pb was loaded onto previously outgassed zone-refined Re filaments with silica gel made from silicic acid (Gerstenberger and Haase 1997). All analyses were made by sequentially peak jumping the ion beams into the central SEM–IC system. Samples were corrected for instrumental mass fractionation using the equal atom ^{202}Pb-^{205}Pb tracer assuming a linear mass fractionation law. Samples are corrected for Pb blank added during the chemical separation according to replicate blanks run during the same session. Pb blanks from the chemistry during this work ranged from 0.2 to 0.6 pg. Samples are also corrected for a 0.1 pg Pb loading blank. Prior to and after each session of mass spectrometry, 0.5 ng of standard SRM-982 were analyzed to

assess the accuracy of measurements. The external reproducibility was 0.032% for $^{207}Pb/^{206}Pb$ (0.467114 ± 0.000149) and 0.104% for $^{206}Pb/^{204}Pb$ (36.735154 ± 0.038175) (Table 2). Final ratios, errors, and error correlations were calculated using an in-house program and PbDat (v. 1.24, Ludwig 1993). Ages were calculated using Isoplot Ex v. 4 (Ludwig 2003), decay constants of Jaffey et al. (1971), and a natural $^{238}U/^{235}U$ ratio of 137.786 (Connelly et al. 2012). All isotope data for samples as well as progressive dissolution steps are reported in full in Table 3.

Results

Mineralogy and Petrography

The four chondrules selected for this study (C1, C2, C3, and C4) are approximately 1 cm in diameter and free from metal. They all exhibit a nonporphyritic texture and are very fine grained. Unlike nebular barred textured chondrules, they lack a surrounding olivine rim. The mineralogy for the four chondrules is identical and consists of olivine, sub-Ca pyroxene, high-Ca pyroxene, anorthite-rich mesostasis, and rare Al-rich sub-Ca pyroxene.

Chondrule C1 is fan- shaped with a mean diameter of 8 mm. It has a radial pyroxene texture with olivine–pyroxene plates varying in size from 1 to 15 μm.

Chondrule C2 has an overall subcircular shape with a mean diameter of 11 mm, but it is deformed by a metal nodule along the margin. It has a barred olivine–pyroxene texture with subparallel fragmented olivine–pyroxene plates with sizes varying from 1 to 15 μm.

Chondrule C3 has a subcircular shape with a mean diameter of 11 mm. It has a barred olivine–pyroxene texture.

Chondrule C4 has a very irregular shape with a mean diameter of 10 mm. It has a barred olivine–pyroxene texture, but much finer grained (sub μm) than other chondrules (Fig. 1).

Absolute Ages

The precision of ages obtained from Pb isochrons is dependent on the precision of the interpolated $^{207}Pb/^{206}Pb$ ratio of Pb_r. High precision requires sufficiently radiogenic fractions with adequate spread to constrain the line and, therefore, the intercept. Highly radiogenic samples provide lower errors on the ages due to a shorter extrapolation to the *y*-axis. Fractions that do not overlap the defined array within their respective stated errors are excluded from the isochron calculation. Isochron relationships for individual chondrules are described below and summarized in Table 4.

Chondrule C1: The Pb isotopic compositions of 13 stepwise dissolution steps were analyzed from this inclusion. The first six dissolution steps show rather unradiogenic Pb with an average $^{206}Pb/^{204}Pb$ of 25, whereas the most radiogenic dissolution step has a $^{206}Pb/^{204}Pb$ of 458. Nine dissolution steps can be successfully regressed to define an isochron corresponding to a $^{207}Pb/^{206}Pb$ age of 4562.39 ± 0.49 Myr (MSWD = 0.70; Fig. 2). Including fraction L11 in the regression does not change the age because of the large errors associated with this fraction.

Europe PMC Funders Author Manuscripts

Chondrule C2: The Pb isotopic compositions of 11 stepwise dissolution steps were analyzed from this inclusion. The first six dissolution steps show rather unradiogenic Pb with an average $^{206}Pb/^{204}Pb$ of 47, whereas the most radiogenic dissolution step has a $^{206}Pb/^{204}Pb$ of 3794. Eight dissolution steps were successfully regressed to define an isochron corresponding to a $^{207}Pb/^{206}Pb$ age of 4562.32 ± 0.52 Myr (MSWD = 0.25; Fig. 3).

Chondrule C3: The Pb isotopic compositions of 11 stepwise dissolution steps were analyzed from this inclusion. The first four dissolution steps show rather unradiogenic Pb with an average $^{206}Pb/^{204}Pb$ of 50, whereas the most radiogenic leachate displays a $^{206}Pb/^{204}Pb$ of 1400. Eight dissolution steps were successfully regressed to define an isochron corresponding to a $^{207}Pb/^{206}Pb$ age of 4562.66 ± 0.43 Myr (MSWD = 0.50; Fig. 4).

Chondrule C4: The Pb isotopic compositions of 13 stepwise dissolution steps were analyzed from this inclusion. The first five dissolution steps show moderately radiogenic Pb with an average $^{206}Pb/^{204}Pb$ of 76, whereas the most radiogenic leachate displays a $^{206}Pb/^{204}Pb$ of 3477. Twelve dissolution steps were successfully regressed to define an isochron corresponding to a $^{207}Pb/^{206}Pb$ age of 4562.50 ± 0.36 Myr (MSWD = 1.5; Fig. 5).

The four isochrons project to a Pb isotopic composition that is less radiogenic than initial Pb isotopic composition of the solar system. Pooling the four ages we obtain a weighted mean age of 4562.49 ± 0.21 Myr, which is our preferred age for chondrule formation (Figs. 6 and 7). If the impact formation model is correct, we expect all dissolution steps from all four chondrules to define a single isochron. Of the 47 dissolution steps, 37 analyses were used to regress the four isochrons, from which 31 can be regressed along a single isochron corresponding to a $^{207}Pb/^{206}Pb$ age of 4562.47 ± 0.22 Myr (MSWD = 1.02; Fig. 6). The 22 most radiogenic leachates with $^{206}Pb/^{204}Pb$ higher than 100 yield a regression line corresponding to a $^{207}Pb/^{206}Pb$ age of 4562.53 ± 0.26 Myr (MSWD = 1.3). This “bulk” isochron Pb-Pb age is indistinguishable from the age defined by the weighted mean of the four ages, which confirms a cogenetic formation.

Initial Pb

The primordial isotope composition of Pb in the solar system was defined by Tatsumoto et al. (1973), based on a troilite component in the Canyon Diablo iron meteorite (PAT: $^{204}Pb/^{206}Pb = 0.10745$ and $^{207}Pb/^{206}Pb = 1.1060$). Chondrules would have initially inherited a low solar $^{238}U/^{204}Pb$ ratio ($\mu \sim 0.14$, Lodders 2003) such that the Pb isotopic composition will not evolve measurably in the first few million years unless the μ-value is increased by Pb devolatilization during thermal processing. Hence, in the simple case of a chondrule formed by a single thermal event, the chondrule will contain a binary mixture of $Pb_i + Pb_r$ and define isochrons that project back to Pb isotopic compositions of PAT. More evolved Pb_i signatures would imply that the μ-value had been raised during at least one thermal event that preceded the final chondrules’ crystallization. Less evolved Pb_i signatures would imply that PAT is not the primordial Pb isotopic signature of the solar system but rather an evolved composition formed in a differentiated high μ parent body prior to core formation. As such, an estimate of the Pb_i for chondrules can provide important information regarding the thermal history of a chondrule and/or the solar system primordial Pb.

The linearity of arrays and the successful collective regression of fractions from all four chondrules confirm a binary system, between radiogenic Pb and a second component with a single isotopic composition. The four isochrons and the collective regression of 31 fractions all project back to a Pb isotopic composition that is significantly below PAT (Fig. 8), raising the possibility that it represents an isotopic composition closer to true primordial Pb than that measured by Tatsumoto et al. (1973). Alternatively, the Gujba chondrules may represent a mixture of Pb_r and terrestrial contaminant Pb, as no analyses lie to the right of Stacey and Kramers' (1975) Pb isotopic composition of averaged modern terrestrial Pb. Therefore, the chondrule data alone cannot differentiate between these two alternatives.

To test whether Gujba contains a more primitive Pb isotopic signature than PAT, we analyzed a Gujba metal nodule assuming that it would essentially be free of U and, therefore, may provide insight into the isotopic composition of Pb_i for this sample. A progressive seven-step dissolution procedure yielded an array that projects from PAT to a value above Stacey and Kramers' (1975) estimate for average modern Pb (Figure 8).

The modern terrestrial Pb composition from Stacey and Kramers (1975) (MT: $^{204}Pb/^{206}Pb$ = 0.05420 and $^{207}Pb/^{206}Pb$ = 0.84228) was defined by averaging the Pb isotopic composition of rocks with various origins (sediments, MORB, OIB, metamorphic) and assumed to represent the average accessible mantle and crust composition today. However, "atmospheric" Pb is more likely to form the terrestrial Pb contaminant in meteorites, such that its isotopic composition may not overlap with the averaged value of Stacey and Kramers (1975). One of the main sources of Pb contamination on Earth's surface arises from the world wide use of tetraethyllead organic compound $(CH_3CH_2)_4Pb$ as an additive in gasoline until the 1970s (Seyferth 2003). The Pb used for the synthesis of tetraethyllead had different origins and, therefore, nonunique Pb isotopic compositions such that atmospheric Pb contamination varies regionally. The meteorite Gujba fell in Yobe, Nigeria where a medical survey (Smith et al. 1996) conducted a study of the Pb isotopic composition of the blood and bone from a Nigerian, which provides a good approximation of the average isotopic composition of atmospheric Pb in this region. The resulting values of $^{204}Pb/^{206}Pb$ = 0.05554 and $^{207}Pb/^{206}Pb$ = 0.86664 lie close to the metal nodule array and are very similar to those obtained for the metal fraction that plots furthest from PAT, the wash fraction ($^{204}Pb/^{206}Pb$ = 0.05650 and $^{207}Pb/^{206}Pb$ = 0.86782). Consequently, we interpret the Gujba metal wash fraction as representative of the anthropogenic Pb component in Nigeria, and conclude that Gujba metal contains two reservoirs of Pb, namely initial Pb (Pb_i) that is represented by PAT and terrestrial contaminant lead (Pb_c) that was acquired in Nigeria. The regression of metal fractions toward an initial Pb isotopic composition similar to PAT indicates that the precursor material had a very low μ-value such that the Pb isotopic composition did not change measurably from T_0 until the impact that formed the chondrules.

The intersection of the chondrule and metal nodule arrays approximately coincides with the estimate of the local modern terrestrial value in Nigeria, indicating that the chondrules are also contaminated with this source of Pb. As we do not observe any chondrule fractions with Pb isotopic compositions less evolved than this modern terrestrial value, we propose that Gujba chondrules are primarily composed of a mixture of pure radiogenic Pb (Pb_r) and local Nigerian terrestrial contaminant lead (Pb_c). The lack of any appreciable initial Pb (Pb_i) in the

chondrules is attributed to an efficient Pb-loss process associated with chondrule formation, commensurate with the high volatility of Pb.

Discussion

Formation by Impact Plume

Krot et al. (2005) invoked an impact-related vapor-melt plume formation model for the CB chondrites to account for their anomalous mineralogical and chemical characteristics and young age they obtained for bulk chondrules. This model predicts that all chondrules should have the same age but this could not be tested with their data. Our new combined absolute Pb-Pb age of 4562.49 ± 0.21 Myr based on four separate Gujba chondrules confirms both a late formation for the Gujba chondrules (offset ~0.8 Myr age from the U-corrected absolute Pb-Pb age of Krot et al. 2005) and that the chondrules formed during a brief interval consistent with a single event. This fully supports the impact-related vapor plume formation model for the Gujba chondrules and, by extension, the CB chondrites as a group. The absence of an initial Pb component (Pb_i) in Gujba chondrules infers that the precursor material experienced extensive devolatilization, consistent with the depletion of volatile and moderately volatile elements noted by Rubin et al. (2003). Using the CAI age of 4567.30 ± 0.16 Myr (Connelly et al. 2012), our new results indicate that Gujba chondrules formed 4.8 ± 0.3 Myr after the formation of the solar system. The youngest nebular chondrule dated thus far yields an age of 4563.67 ± 0.3 Myr (Bollard et al. 2014), such that Gujba chondrules formed 1.2 ± 0.6 Myr later. Collectively, all data for the CB chondrites are fully consistent with an impact-related vapor plume formation model for this group. If the migration of gas giants was the trigger for these hypervelocity collisions, as implied by the Grand Tack model (Walsh et al. 2011), our new data places a precise age on this event.

Offset of Age Relative to the Previous Absolute Pb Age

The four Gujba chondrules analyzed here define a new absolute Pb-Pb age of 4562.49 ± 0.21 Myr. Our age is defined by four similar ages with excellent reproducibility from four single chondrules. Furthermore, the regression of 31 fractions from all four chondrules collectively yields the same age. Our new age is 0.81 ± 0.55 Myr older than the previous absolute Pb age of Krot et al. (2005), after correcting their age for the uranium isotopic composition. Given the consistency in ages derived by the two groups for other samples (e.g., SAH 99555—Amelin [2008] and Connelly et al. [2008]), we have no explanation for the offset between these two ages. Another issue arises with the CB_b Hammadah al Hamra 237 (HaH237), which Krot et al. (2005) also dated in the same project as Gujba. Their absolute Pb-Pb age, once corrected for uranium, is 4561.8 ± 0.9 Myr. But if a similar bias between their Pb-Pb dating procedure and our Gujba age exists, we could apply a similar offset of ~ 0.8 Myr for HaH237 chondrules making them as old as our age for Gujba chondrules. Consequently, the suggestion of formation of both CB_a and CB_b chondrites during the same impact event would remain valid.

Comparison with Short-Lived Radionuclide Chronometers

Comparing our new absolute Pb-Pb age of 4562.49 ± 0.21 Myr with the ages determined with extinct radionuclide chronometers, we observe overall consistency with age offsets

Europe PMC Funders Author Manuscripts

Europe PMC Funders Author Manuscripts

ranging from −0.78 to +0.74 Myr, but all overlapping within the stated errors (Fig. 9; Table 5). The Al-Mg is not relevant as the young age formation, almost seven half-lives of ^{26}Al, implies that most ^{26}Al must had decayed away by this time. This is confirmed by Olsen et al. (2013) who observed no resolvable ^{26}Mg excess in Gujba chondrules.

The ^{53}Mn-^{53}Cr System—The most common time anchors used for the Mn-Cr system are the fine-grained angrite D'Orbigny and the coarse-grained angrite LEW 86010. Although a range of initial ^{53}Mn/^{55}Mn ratios exist for D'Orbigny, the highest precision value of (3.24 ± 0.04) × 10^{-6} by Glavin et al. (2004) is the most commonly cited initial ratio. Two initial values for LEW 86010 exist, namely (1.25 ± 0.07) × 10^{-6} (Lugmair and Shukolyukov 1998) and (1.40 ± 0.07) × 10^{-6} (Nyquist et al. 1994) where both are corrected for spallation reactions recorded by this meteorite. Of these two values, the initial ratio from Lugmair and Shukolyukov (1998) is the most commonly cited value as an anchor. Mn-Cr data for Gujba chondrules and metal presented by Yamashita et al. (2010) return ages of 4563.27 ± 0.91 and 4562.52 ± 1.15 Myr relative to the time anchors D'Orbigny and LEW 86010, respectively. These ages are offset from our Pb-Pb age for Gujba by 0.78 ± 0.94 (relative to D'Orbigny) and 0.03 ± 1.16 Myr (relative to LEW 86010). Although both angrite anchors provide Mn-Cr ages for Gujba that overlap our Pb-Pb age, the estimate based on D'Orbigny requires that the highest initial ^{53}Mn/^{55}Mn ratio of those available is used as a reference. The full range of ^{53}Mn/^{55}Mn ratios available for D'Orbigny ([2.83 ± 0.25] × 10^{-6}, Nyquist et al. [2003]; [2.84 ± 0.24] × 10^{-6}, Sugiura et al. [2005]; [3.24 ± 0.04] × 10^{-6}, Glavin et al. [2004]; [3.20 ± 0.21] × 10^{-6}, Yin et al. [2009]; [3.44 ± 0.29] × 10^{-6} and [3.60 ± 0.39] × 10^{-6}, McKibbin et al. [2013]) which was critically reviewed by McKibbin et al. (2013), corresponds to an age range of 1.29 ± 1.07 Myr with some estimates outside of our new Pb-Pb age for Gujba. Conversely, only the lowest value for LEW 86010 overlaps with our new Pb-Pb age.

The complexity arising from the use of D'Orbigny or other angrites with well-constrained Mn-Cr data as anchors becomes even more obvious when all available Mn-Cr data for angrites is plotted against their respective Pb-Pb ages (Fig. 10). This figure also displays two ^{53}Mn decay lines, one anchored to the Gujba value and the other to the Glavin et al. (2004) value of D'Orbigny. The agreement between Gujba and lowest initial estimate for LEW 86010 is clear on this diagram, as is the discordance of NWA 4801, NWA 4590, SAH 99555, NWA 1670, some of the D'Orbigny analyses, and the highest ratio for LEW86010. The reason for the discordance between these samples and the Gujba decay line is uncertain but may include different closure temperatures and slow cooling. The closure temperature for Pb diffusion in pyroxene is estimated around 700 °C and about 600 °C for the closure of Cr diffusion in olivine (Amelin 2008), the two most important phases for the Pb-Pb and Mn-Cr dating methods, respectively. The new precise Pb-Pb age for Gujba and its consistent Mn-Cr systematic displayed in Yamashita et al. (2010) suggests that Gujba may serve as a better primary anchor than any of the angrites. This ideally would require a second study to confirm the result of Yamashita et al. (2010).

The ^{182}Hf-^{182}W System—Gujba metal yields a Hf-W age of 4562.2 ± 2.4 (Kleine et al. 2005) when this system is anchored by calcium-aluminum inclusions with an age of 4567.30 ± 0.16 Ma (Connelly et al. 2012). Although the errors for this age are too large to critically

evaluate the concordance between the Hf-W and Pb-Pb age in detail, the two ages are in agreement and, therefore, support the assumption of a homogeneous distribution of ^{182}Hf within the inner protoplanetary disk over its lifetime. As such, the Hf-W is considered to be a viable chronometer for dating early solar system objects and events. The cogenetic metal and silicates formed within a plume comprising a single reservoir would make Gujba an ideal time anchor or, at least, a valuable secondary reference for the Hf-W system, especially if a more precise estimate of the initial ^{182}Hf/^{180}Hf ratio could be measured for this meteorite.

The ^{129}I-^{129}Xe System—The I-Xe age obtained by Gilmour et al. (2009) on one of nine Gujba chondrules corresponds, after uranium correction for the interpolated absolute age of Shallowater, to an age of 4563.23 ± 1.30 Myr, which is 0.74 ± 1.32 Myr older than our Pb-Pb age for Gujba chondrules. Working with an uncorrected age of Shallowater, Pravdivtseva et al. (2014) reported an I-Xe age for Gujba that was 1.5 Myr older (i.e., 4564.2 ± 1.2 Myr) than the Pb-Pb age for Gujba by Krot et al. (2005). Given the concordance with our new age, any explanations of the former apparent discordance are no longer necessary or valid.

Pravdivtseva et al. (2014) also successfully obtained an I-Xe age for one of four CB_b HaH237 chondrules, corresponding to a closure age of 0.29 ± 0.32 Myr after Shallowater, which corresponds to a U-corrected age of 4561.01 ± 0.87 Myr for this chondrule. This age is 1.48 ± 0.90 Myr younger than our Gujba chondrule age. This discrepant age outside of errors contradicts the assumed contemporaneous formation of CB_a and CB_b chondrites in a single impact event. We exclude disturbance of the I-Xe systematics by later shock metamorphism on the CB parent body as an explanation for the different ages, as the retention of radiogenic ^{129}Xe has a higher closure temperature (~1300–1400 °C) than for closure of the Pb-Pb system (i.e., ~700 °C).

The age offset for the CB_a and CB_b samples may be explained by an inhomogeneous ^{129}I/^{127}I within the impact plume due to primary differences between the two colliding bodies. This may be possible in the dynamical model envisioned by Condie (2012), where the plume would be structured with numerous convection cells that would have mixed and sorted the material to eventually generate the different CB_a and CB_b meteorites. We hypothesize that an iodine-carrier phase with higher ^{129}I/^{127}I was concentrated in the convection cell that produced the CB_b chondrules.

Given the well-behaved I-Xe systematics in Shallowater that yields consistent isochrons (Gilmour et al. 2006), this meteorite has been adopted as the primary I-Xe standard to calibrate the irradiation of ^{127}I to ^{128}Xe despite the lack of a Pb-Pb age for this sample. Assuming the I-Xe data for Gujba is correct and adopting our absolute Pb age of Gujba as a reference, the I-Xe interval of −1.93 ± 0.88 Myr for Gujba relative to the Shallowater aubrite corresponds to an absolute age of 4560.56 ± 0.91 Myr for Shallowater, which is 0.7 ± 1.2 Myr younger than the published age (Gilmour et al. 2009) that we have corrected for the U isotopic composition of 137.786. While these age estimates overlap, the large total spread of inferred absolute ages makes clear the need to directly date the Shallowater aubrite if it continues to serve as the primary standard for the I-Xe system. Alternatively, Iizuka et al.

Europe PMC Funders Author Manuscripts

(2014) suggested the achondrite Ibitira, an unbrecciated monomict eucrite, may serve as a more suitable irradiation standard for the I-Xe system.

Gujba as a Possible Use as Time Anchor?

High-precision Pb-Pb ages of angrites are widely used as reference points for extinct radionuclide chronology, but it is important to cross-reference the angrite-based time scale with a different group of meteorites to determine whether the extinct radionuclides were homogeneously distributed in the early solar system (Wadhwa et al. 2009; Bouvier et al. 2011; Kita et al. 2013). The apparent formation of the CB_a Gujba chondrite in a single-stage impact plume implies an isotopically uniform reservoir and subsequent simultaneous resetting of all systematics, with the possible exception of the I-Xe system. Given our new precise absolute Pb-Pb age for Gujba chondrules, the concordancy of the available ages and the large amount of material available (~100 kg), Gujba has the potential to serve as either a secondary reference anchor or, in some cases, a better primary reference anchor than that currently employed.

On a cautionary note, evidence of late-stage impact or impacts has been suggested by shock features (Weisberg and Kimura 2010; Garvie et al. 2011) and there is evidence for reheating (Srinivasan et al. 2014). While the evidence for shock may be irrefutable, the concordancy of the chronometers suggests that element remobilization was minimal during these events. As such, we consider Gujba as a viable anchor to map at least the ^{53}Mn-^{53}Cr and ^{182}Hf-^{182}W and, perhaps the ^{129}I-^{129}Xe system, onto the absolute time scale using our precise absolute Pb-Pb age. This ideally would require a multi-isotopic study on one chondrule that provided a precise Pb-Pb age, to ensure the best correlation between all systematics.

A Proxy for Accretion Disk Timescales

The absence of any interchondrule fine-grained matrix or fine-grained rims around chondrules testifies to their formation in a dust-free environment. Combined with their young age, this environment is consistent with a “debris disk” when the fine-grained dust is mostly cleared. However, these characteristics alone may not be uniquely indicative of formation in a debris disk. Instead, they could be associated with the transition disk phase, where disk dispersion occurs either by photoevaporation, dust settling, or planet formation (Williams and Cieza 2011; Kim et al. 2013). However, the hypervelocity collision ($v_{imp} \gg v_{esc}$) of 10–50 km s^{-1} involved in Gujba formation may only be possible with bodies having a very high eccentric orbit, a feature we expect during giant planets’ migration as predicted by the Grand Tack model (Walsh et al. 2011). Most of the gas should have dissipated by this time to prevent any damping effect by gas drag. If our interpretation of a dust free disk is correct, our age places a lower age limit on the lifetime of the gas and dust-rich protoplanetary disk at 4562.49 ± 0.21 Myr, implying a maximum lifetime of the solar system’s nebular disk at 4.8 ± 0.3 Myr. A lower limit for the age of this disk comes from the youngest nebular chondrule with an age of 4563.67 ± 0.3 Myr (Bollard et al. 2014) or 3.6 ± 0.5 Myr after the protoplanetary disk was established. This provides the time of the transition from a dusty, nebular stage to a debris disk at 3.1–5.1 Myr after T_0, which includes the full range of uncertainties. This transitional timeframe is in excellent agreement with

observations. From Spitzer surveys, Currie and Sicilia-Aguilar (2011) showed that for 0.5–1.4 $M_{\odot}$ stars, the percentage of disks in the transitional phase increases from ~ 15% to 20% at 1–2 Myr to ≥50% at 5–8 Myr, with a derived mean transitional disk lifetime close to ~ 1 Myr.

In defining the statistics on the lifetime of protoplanetary disks based on observational data, they utilize the so-called “Haisch-Lada” plot (Haisch and Lada 2001; Mamajek 2009), which displays the fraction of stars with primordial disks remaining as a function of mean cluster age. Such analyses show that by ca. 8 Myr, only 5% of the disks will still possess an accretion disk. As noted by Yasui et al. (2014), these statistics include all detected cluster members and, thus, the estimated lifetime is primarily for low-mass stars considering the characteristic mass of the initial mass function (IMF) (~ 0.2–0.3 solar mass, $M_{\odot}$; Chabrier 2003; Bochanski et al. 2010). For higher mass stars like the Sun, the debris disk forms earlier, with a clear distinction between low-mass stars (~ 0.1–1.5 $M_{\odot}$) and intermediate-mass stars (~ 1.5–7 $M_{\odot}$) (Kennedy and Kenyon 2009; Mamajek 2009; Yasui et al. 2014). Yasui et al. (2014) obtained a stellar mass dependence of the disk lifetime proportional to a power-law function of stellar mass equal to $M_{*}^{-0.8\pm0.7}$. Consequently, the corresponding disk lifetime for stellar masses of 0.3 $M_{\odot}$ would be 2.6 times longer than the lifetime of a 1 $M_{\odot}$ disk. These values are purely qualitative as there are large uncertainties on the mass-dependent function, requiring more direct observations of 1 $M_{\odot}$ stars. Regardless, this analysis is compatible with our estimates for the lifetime of the disk based on Pb-Pb ages of nebular chondrules and Gujba.

Therefore, we suggest a timeframe for the solar protoplanetary disk evolution based on the CAI formation (4567.30 ± 0.16 Myr; Connelly et al. 2012), the youngest nebular chondrule (4563.67 ± 0.3 Myr; Bollard et al. 2014), and Gujba (4562.49 ± 0.21 Myr). The protoplanetary lifetime is estimated at 4.8 ± 0.3 Myr, with the following stages (1) primordial active disk lasting for 3.6 ± 0.5 Myr, (2) transitional protoplanetary disk lasting 1.2 ± 0.6 Myr followed by, (3) the debris disk.

Conclusions

The main motivation for this study was to confirm the young age of formation of the CB_a Gujba chondrites and to determine the age range of single chondrules to test the impact formation model of Krot et al. (2005). We have undertaken absolute Pb-Pb dating of four single chondrules that yield indistinguishable ages that collectively define a precise weighted mean age of 4562.49 ± 0.21 Myr. This age is concordant with ages obtained with ^{53}Mn-^{53}Cr, ^{182}Hf-^{182}W, and ^{129}I-^{129}Xe short-lived radiochronometers indicating that these shortlived radionuclides were homogeneously distributed across the accretion regions of the relevant parent bodies within the resolution of the current measurements. The short time span of formation and rapid cooling implied by the simultaneous closure of all chronometers supports the impact plume formation model. Given the brief formation period, we propose the use of Gujba as a viable anchor for at least the ^{53}Mn-^{53}Cr and ^{182}Hf-^{182}W systems and, perhaps the ^{129}I-^{129}Xe system. The impact model scenario also implies a formation in a planetary setting, such that the age for Gujba sets an upper limit of ~4.8 Myr for the lifetime of the protoplanetary disk and the timing of planet formation.

Europe PMC Funders Author Manuscripts

Acknowledgments

Funding for this project was provided by grants from the Danish National Research Foundation (#DNRF97) and from the European Research Council (ERC Consolidator grant agreement 616027-STARDUST2ASTEROIDS) to M.B.

References

Amelin Y. U-Pb ages of angrites. Geochimica et Cosmochimica Acta. 2008; 72:221–232.

Amelin Y, Ghosh A, Rotenberg E. Unravelling evolution of chondrite parent asteroids by precise U-Pb dating and thermal modeling. Geochimica et Cosmochimica Acta. 2005; 69:505–518.

Asphaug E, Jutzi M, Movshovitz N. Chondrule formation during planetesimal accretion. Earth and Planetary Science Letters. 2011; 308:369–379.

Bochanski JJ, Hawley SL, Covey KR, West AA, Reid N, Golimowski DA, Ivezic Ž. The luminosity and mass functions of low-mass stars in the galactic disk: II. The field. The Astronomical Journal. 2010; 139:2679–2699.

Boley AC, Durisen RH. Gravitational instabilities, chondrule formation, and the FU orionis phenomenon. The Astrophysical Journal. 2008; 685:1193–1209.

Bollard, J.; Connelly, JN.; Bizzarro, M. The absolute chronology of the early solar system revisited. Meteoritics & Planetary Science. 77th Annual Meteoritical Society Meeting; 2014. (abstract #5234)

Boss AP, Graham JA. Clumpy disk accretion and chondrule formation. Icarus. 1993; 106:168–178.

Boss AP, Durisen RH. Chondrule-forming shock fronts in the solar nebula: A possible unified scenario for planet and chondrite formation. The Astrophysical Journal. 2005; 621:L137–L140.

Bouvier A, Spivak-Birndorf L, Brennecka GA, Wadhwa M. New constraints on early solar system chronology from Al–Mg and U-Pb isotope systematics in the unique basaltic achondrite Northwest Africa 2976. Geochimica et Cosmochimica Acta. 2011; 75:5310–5323.

Brazzle RH, Pravdivtseva OV, Meshik AP, Hohenberg CM. Verification and interpretation of the I-Xe chronometer. Geochimica et Cosmochimica Acta. 1999; 63:739–760.

Brennecka GA, Wadhwa M. Uranium isotope compositions of the basaltic angrite meteorites and the chronological implications for the early solar system. Proceedings of the National Academy of Sciences of the United States of America. 2012; 109:9299–9303. [PubMed: 22647606]

Brennecka GA, Weyer S, Wadhwa M, Janney PE, Zipfel J, Anbaret AD. $^{238}U/^{235}U$ variations in meteorites: Extant ^{247}Cm and implications for Pb-Pb dating. Science. 2010; 327:449–451. [PubMed: 20044543]

Campbell AJ, Humayun M, Weisberg MK. Siderophile element constraints on the formation of metal in the metal-rich chondrites Bencubbin, Weatherford, and Gujba. Geochimica et Cosmochimica Acta. 2002; 66:647–660.

Chabrier G. Galactic stellar and substellar initial mass function. Publications of the Astronomical Society of the Pacific. 2003; 115:763–795.

Ciesla FJ, Hood LL, Weidenschilling SJ. Evaluating planetesimal bow shocks as sites for chondrule formation. Meteoritics & Planetary Science. 2004; 39:1809–1821.

Condie, C. The use of experimental petrology to generate an impact model for formation of the unique CB_b chondrules. Ph.D. thesis; Rutgers University, New Brunswick, New Jersey, USA: 2012.

Connelly JN, Bizzarro M. Pb-Pb dating of chondrules from CV chondrites by progressive dissolution. Chemical Geology. 2009; 259:143–151.

Connelly JN, Bizzarro M, Thrane K, Baker JA. The Pb–Pb age of Angrite SAH 99555 revisited. Geochimica et Cosmochimica Acta. 2008; 72:4813–4824.

Connelly JN, Bizzarro M, Krot AN, Nordlund Å, Wielandt D, Ivanova MA. The absolute chronology and thermal processing of solids in the solar protoplanetary disk. Science. 2012; 338:651. [PubMed: 23118187]

Connolly HC Jr, Desch SJ. On the origin of the “kleine Kugelchen” called chondrules. Chemie der Erde/Geochemistry. 2004; 64:95–125.

Connolly HC Jr, Love SG. The formation of chondrules: Petrologic tests of the shock wave model. Science. 1998; 280:62–67. [PubMed: 9525858]

Connolly, HC., Jr; Desch, SJ.; Ash, RD.; Jones, RH. Transient heating events in the protoplanetary nebula. Meteorites and the early solar system II. Lauretta, DS.; McSween, HY., editors. Tucson, Arizona: University of Arizona Press; 2006. p. 383-397.

Currie T, Sicilia-Aguilar A. The transitional protoplanetary disk frequency as a function of age: Disk evolution in the Coronet Cluster, Taurus, and other 1–8 Myr-old regions. The Astrophysical Journal. 2011; 732:24–59.

Desch SJ, Morrris MA, Connolly HC Jr, Boss AP. The importance of experiments: Constraints on chondrule formation models. Meteoritics & Planetary Science. 2012; 47:1139–1156.

Fedkin, AV.; Grossman, L.; Campbell, AJ.; Humayunet, M. CB chondrites could have formed in an impact plume. 44th Lunar and Planetary Science Conference. CD-ROM; 2013. (abstract #2309)

Fedkin, AV.; Grossman, L.; Humayun, M.; Simon, SB.; Campbell, AJ. Impact formation of CB chondrites: The metal-rich body had a silicate mantle. 45th Lunar and Planetary Science Conference. CD-ROM; 2014. (abstract #2153)

Garvie LAJ, Németh P, Buseck PR. Diamond, bucky-diamond, graphite-diamond, Al-silicate, and stishovite in the Gujba CB chondrite. Meteoritics & Planetary Science. 2011; 46:A75. (abstract #5227).

Gerstenberger H, Haase G. A highly effective emitter substance for mass spectrometric Pb isotope ratio determinations. Chemical Geology. 1997; 136:309–312.

Gilmour JD, Pravdivtseva OV, Busfield A, Hohenberg CM. The I-Xe chronometer and the early solar system. Meteoritics & Planetary Science. 2006; 41:19–31.

Gilmour JD, Crowther SA, Busfield A, Holland G, Whitby JA. An early I-Xe age for CB chondrite chondrule formation, and a re-evaluation of the closure age of Shallowater enstatite. Meteoritics & Planetary Science. 2009; 44:573–579.

Glavin DP, Kubny A, Jagoutz E, Lugmair GW. Mn-Cr isotope systematics of the D'Orbigny angrites. Meteoritics & Planetary Science. 2004; 39:693–700.

Goldmann A, Brennecka G, Noordmann J, Weyer S, Wadhwa M. The uranium isotopic composition of the Earth and the solar system. Geochimica et Cosmochimica Acta. 2015; 148:145–158.

Gooding JL, Keil K. Relative abundances of chondrule primary textural types in ordinary chondrites and their bearing on chondrule formation. Meteoritics. 1981; 16:17–43.

Grossman, JN.; Rubin, AE.; Nagahara, H.; King, EA. Properties of chondrules. Meteorites and the early solar system. Lauretta, DS.; McSween, HY., editors. Tucson, Arizona: University of Arizona Press; 1988. p. 619-659.

Haisch KE, Lada E. Disk frequencies and lifetimes in young clusters. The Astrophysical Journal. 2001; 553:L153–L156.

Hewins RH. Chondrules. Annual Review of Earth and Planetary Sciences. 1997; 25:61–83.

Hewins, RH.; Connolly, HC.; Lofgren, GE., Jr; Libourel, G. Experimental constraints on chondrule formation. Chondrites and the protoplanetary disk. Krot, AN.; Scott, ERD.; Reipurth, B., editors. Vol. 341. San Francisco, California: Astronomical Society of the Pacific; 2005. p. 286-316.

Holden NE. Total half-lives for selected nuclides. Pure and Applied Chemistry. 1990; 62:941–958.

Holst JC, Olsen MB, Paton C, Nagashima K, Schiller S, Wielandt D, Larsen KK, Connelly JN, Jørgensen JK, Krot AN, Nordlund Å, et al. ^{182}Hf–^{182}W age dating of a ^{26}Al-poor inclusion and implications for the origin of short-lived radioisotopes in the early solar system. Proceedings of the National Academy of Sciences. 2013; 110:8819–8823.

Hood LL. Thermal processing of chondrule and CAI precursors in planetesimal bow shocks. Meteoritics & Planetary Science. 1998; 33:97–107.

Hood, LL.; Ciesla, FJ.; Weidenschilling, SJ. Chondrule formation in planetesimal bow shocks: Heating and cooling rates. Chondrites and the protoplanetary disk. Krot, AN.; Scott, ERD.; Reipurth, B., editors. Vol. 341. San Francisco, California: Astronomical Society of the Pacific; 2005. p. 873-882.

Hood LL, Ciesla FJ, Artemieva NA, Marzari F, Weidenschilling SJ. Nebular shock waves generated by planetesimals passing through Jovian resonances: Possible sites for chondrule formation. Meteoritics & Planetary Science. 2009; 44:327–342.

Iizuka T, Amelin Y, Kaltenbach A, Koefoed P, Stirlinget CH. U-Pb systematics of the unique achondrite Ibitira: Precise age determination and petrogenetic implications. Geochimica et Cosmochimica Acta. 2014; 132:259–273.

Jaffey AH, Flynn KF, Glendenin LE, Bentley WC, Essling AM. Precision measurements of halflives and specific activities of ^{235}U and ^{238}U. Physical Review C. 1971; 4:1889–1906.

Johnson BJ, Minton DA, Melosh HJ, Zuber MT. Impact jetting as the origin of chondrules. Nature. 2015; 517:339–341. [PubMed: 25592538]

Jones, RH.; Lee, T.; Connolly, HC., Jr; Love, SG.; Shang, H. Formation of chondrules and CAIs: Theory vs observation. Protostars and planets IV. Mannings, V.; Boss, AP.; Russell, SS., editors. Tucson, Arizona: University of Arizona Press; 2000. p. 927-962.

Jones, RH.; Grossman, JN.; Rubin, AE. Chemical, mineralogical and isotopic properties of chondrules: Clues to their origin. Chondrites and the protoplanetary disk. Krot, AN.; Scott, ERD.; Reipurth, B., editors. Vol. 341. San Francisco, California: Astronomical Society of the Pacific; 2005. p. 251-284.

Joung MKR, Mac Low M-M, Ebel DS. Chondrule formation and protoplanetary disk heating by current sheets in nonideal magnetohydrodynamic turbulence. The Astrophysical Journal. 2004; 606:532–541.

Kennedy GM, Kenyon SJ. Stellar mass dependent disk dispersal. The Astrophysical Journal. 2009; 695:1210–1226.

Kim KH, Watson DM, Manoj P, Forrest WJ, Najita J, Furlan E, Sargent B, Espaillat C, Muzerolle J, Megeath T, Calvet N, et al. Transitional disks and their origins: An infrared spectroscopic survey of Orion A. The Astrophysical Journal. 2013; 769:149.

Kita NT, Yin QZ, MacPherson GJ, Ushikubo T, Jacobsen B, Nagashima K, Kurahashi E, Krot AN, Jacobsen SB. ^{26}Al–^{26}Mg isotope systematics of the first solids in the early solar system. Meteoritics & Planetary Science. 2013; 48:1383–1400.

Kleine T, Mezger K, Münker C, Palme H, Bischoff A. ^{182}Hf-^{182}W isotope systematics of chondrites, eucrites and Martian meteorites: Chronology of core formation and mantle differentiation in Vesta and Mars. Geochimica et Cosmochimica Acta. 2004; 68:2935–2946.

Kleine T, Mezger K, Palme H, Scherer E, Münker C. Early core formation in asteroids and late accretion of chondrite parent bodies: Evidence from ^{182}Hf-^{182}W in CAIs, metal-rich chondrites and iron meteorites. Geochimica et Cosmochimica Acta. 2005; 69:5805–5818.

Krot, AN.; McKeegan, KD.; Meibom, A.; Keil, K. Oxygen-isotope compositions of condensate CAIs and chondrules in the metal-rich chondrites Hammadah Al Hamra 237 and QUE 94411. 64th Annual Meteoritical Society Meeting; 2001. (abstract #5105)

Krot AN, Meibom A, Weisberg MK, Keil K. The CR chondrite clan: Implications for early solar system processes. Meteoritics & Planetary Science. 2002; 37:1451–1490.

Krot AN, Amelin Y, Cassen P, Meibom A. Young chondrules in CB chondrites from a giant impact in the early solar system. Nature. 2005; 436:989–992. [PubMed: 16107841]

Krot AN, Amelin Y, Bland P, Ciesla FJ, Connelly J, Davis AM, Huss GR, Hutcheon ID, Makide K, Nagashima K, Nyquist LE, et al. Origin and chronology of chondritic components: A review. Geochimica et Cosmochimica Acta. 2009; 73:4963–4997.

Kruijer TS, Fischer-Gödde M, Kleine T, Sprung P, Leya I, Wieler R. Neutron capture on Pt isotopes in iron meteorites and the Hf–W chronology of core formation in planetesimals. Earth and Planetary Science Letters. 2013; 361:162–172.

Kruijer TS, Touboul M, Fischer-Gödde M, Bermingham KR, Walker RJ, Kleine T. Protracted core formation and rapid accretion of protoplanets. Science. 2014a; 344:1150–1154. [PubMed: 24904163]

Kruijer TS, Kleine T, Fischer-Gödde M, Burkhardt C, Wieler R. Nucleosynthetic W isotope anomalies and the Hf–W chronometry of Ca–Al–rich inclusions. Earth and Planetary Science Letters. 2014b; 403:317–327.

Lauretta, DS.; Nagahara, H.; Alexander, CMO'D. Petrology and origin of ferromagnesian silicate chondrules. Meteorites and the early solar system II. Lauretta, DS.; McSween, HY., editors. Tucson, Arizona: University of Arizona Press; 2006. p. 431-459.

Lodders K. Solar system abundances and condensation temperatures of the elements. The Astrophysical Journal. 2003; 591:1220–1247.

Ludwig KR. PBDAT: A computer program for processing Pb–U–Th isotope data. United States Geological Survey Open File Report. 1993:88–524.

Ludwig KR. Isoplot/Ex version 3.00, a geochronological toolkit for Microsoft Excel. Berkeley Geochronology Center Special Publ. 4. May 30.2003

Lugmair GW, Galer SJG. Age and isotopic relationships among the angrites Lewis Cliff 86010 and Angra dos Reis. Geochimica et Cosmochimica Acta. 1992; 56:1673–1694.

Lugmair GW, Shukolyukov A. Early solar system timescales according to ^{53}Mn–^{53}Cr systematics. Geochimica et Cosmochimica Acta. 1998; 62:2863–2886.

Mamajek, EE. Initial conditions of planet formation: Lifetimes of primordial disks. AIP Conference Proceedings; 2009. p. 3-10.

McKibbin SJ, Ireland TR, Amelin Y, Holden P, Sugiura N. A re-evaluation of the Mn–Cr systematics of olivine from the angrite meteorite D'Orbigny using Secondary Ion Mass Spectrometry. Geochimica et Cosmochimica Acta. 2013; 123:181–194.

Nakamoto, T.; Hayashi, MR.; Kita, NT.; Tachibana, S. Chondrule-forming shock waves in the solar nebula by X-ray flares. Chondrites and the protoplanetary disk. Hewins, RH.; Jones, RH.; Scott, ERD., editors. Vol. 341. Cambridge, UK: Cambridge University Press; 2005. p. 883-892.

Nelson, AF.; Ruffert, M. A proposed origin for chondrule-forming shocks in the solar nebula. Chondrites and the protoplanetary disk. Hewins, RH.; Jones, RH.; Scott, ERD., editors. Vol. 341. Cambridge, UK: Cambridge University Press; 2005. p. 903-912.

Nyquist LE, Bansal B, Wiesmann H, Shih C-Y. Neodymium, strontium and chromium isotopic studies of the LEW86010 and Angra dos Reis meteorites and the chronology of the angrite parent body. Meteoritics. 1994; 29:855–872.

Nyquist, LE.; Shih, CY.; Wiesmann, H.; Mikouchi, T. Fossil ^{26}Al and ^{53}Mn in D'Orbigny and Sahara 99555 and the timescale for angrite magmatism. 34th Lunar and Planetary Science Conference. CD-ROM; 2003. (abstract #1388)

Olsen MB, Schiller M, Krot AN, Bizzarro M. Magnesium isotope evidence for single stage formation of cb chondrules by colliding planetesimals. The Astrophysical Journal Letters. 2013; 776:L1.

Pravdivtseva, O.; Meshik, A.; Hohenberg, CM.; Krot, AN.; Amelin, Y. I-Xe age of a non-porphyritic magnesian chondrule from the Hammadah al Hamra 237 CB carbonaceous chondrite: Validation of absolute I-Xe ages. 45th Lunar and Planetary Science Conference. CD-ROM; 2014. (abstract #2456)

Rubin AE. Petrologic, geochemical and experimental constraints on models of chondrule formation. Earth-Science Reviews. 2000; 50:3–27.

Rubin AE. The origin of chondrules and chondrites. Geochimica et Cosmochimica Acta. 2005; 69:4745–4746.

Rubin AE. Physical properties of chondrules in different chondrite groups: Implications for multiple melting events in dusty environments. Geochimica et Cosmochimica Acta. 2010; 74:4807–4828.

Rubin AE, Kallemeyn GW, Wasson JT, Clayton RN, Mayeda TK, Grady M, Verchovsky AB, Eugster O, Lorenzetti S. Formation of metal and silicate globules in Gujba: A new Bencubbin-like meteorite fall. Geochimica et Cosmochimica Acta. 2003; 67:283–3298.

Ruzmaikina TV, Ip WH. Chondrule formation in radiative shock. Icarus. 1994; 112:430–447.

Salmeron R, Ireland TR. Formation of chondrules in magnetic winds blowing through the proto-asteroid belt. Earth and Planetary Science Letters. 2012; 327:61–67.

Sanders, IS. A chondrule-forming scenario involving molten planetesimals. Chondrules and the protoplanetary disk. Hewins, RH.; Jones, RH.; Scott, ERD., editors. Cambridge, UK: Cambridge University Press; 1996. p. 327-334.

Sanders, IS.; Taylor, GJ. Implications of Al in nebular dust: Formation of chondrules by disruption of molten planetesimals. Chondrites and the protoplanetary disk. Krot, AN.; Scott, ERD.; Reipurth, B., editors. Vol. 341. San Francisco, California: Astronomical Society of the Pacific; 2005. p. 915-932.

Shukolyukov, A.; Lugmair, GW. Mn-Cr chronology of eucrite CMS 04049 and angrite NWA 2999. 39th Lunar and Planetary Science Conference. CD-ROM; 2008. (abstract #2094)

Shukolyukov, A.; Lugmair, GW.; Irving, AJ. Mn-Cr isotope systematics of angrite Northwest Africa 4801. 40th Lunar and Planetary Science Conference. CD-ROM; 2009. (abstract #1381)

Seyferth D. The rise and fall of tetraethyllead. 2. Organometallics. 2003; 22:5154–5178.

Shu FH, Shang H, Glassgold AE, Lee T. X-rays and fluctuating X-winds from protostars. Science. 1997; 277:1475–1479.

Smith DR, Osterloh JD, Flegal AR. Use of endogenous, stable lead isotopes to determine release of lead from the skeleton. Environmental Health Perspectives. 1996; 104:60–66. [PubMed: 8834863]

Srinivasan, P.; Jones, RH.; Brearley, AJ. Thermal histories of CB meteorites: Evidence of reheating from CR-rich sulfides. 45th Lunar and Planetary Science Conference. CD-ROM; 2014. (abstract #2286)

Stacey JS, Kramers JD. Approximation of terrestrial lead isotope evolution by a two-stage model. Earth and Planetary Science Letters. 1975; 26:207–221.

Sugiura N, Miyazaki A, Yanai K. Widespread magmatic activities on the angrite parent body at 4562 Ma ago. Earth, Planets and Space. 2005; 57:e13–e16.

Tatsumoto M, Knight RJ, Allègre CJ. Time differences in the formation of meteorites as determined from the ratio of lead-207 to lead-206. Science. 1973; 180:1279–1283. [PubMed: 17759123]

Urey HC. Parent bodies of the meteorites and the origin of chondrules. Icarus. 1967; 7:350–359.

Urey HC, Craig H. The composition of the stone meteorites and the origin of the meteorites. Geochimica et Cosmochimica Acta. 1953; 4:36–82.

Vockenhuber C, Oberli F, Bichler M, Ahmad I, Quitté G, Meier M, Halliday AN, Lee D-C, Kutschera W, Steier P, Gehrke RJ, et al. New half-life measurement of Hf^{182}: Improved chronometer for the early solar system. Physical Review Letters. 2004; 93:172–501.

Wadhwa M, Amelin Y, Bogdanovski O, Shukolyukovc A, Lugmair GW, Janney P. Ancient relative and absolute ages for a basaltic meteorite: Implications for timescales of planetesimal accretion and differentiation. Geochimica et Cosmochimica Acta. 2009; 73:5189–5201.

Walsh KJ, Morbidelli A, Raymond SN, O'Brien DP, Mandell AM. A low mass for Mars from Jupiter's early gas-driven migration. Nature. 2011; 475:206–209. [PubMed: 21642961]

Weisberg MK, Kimura H. Petrology and Raman spectroscopy of high pressure phases in the Guijba CB chondrite and the shock history of the CB parent body. Meteoritics & Planetary Science. 2010; 45:873–884.

Williams JP, Cieza LA. Protoplanetary disks and their evolution. Annual Review of Astronomy and Astrophysics. 2011; 49:67–117.

Yamashita K, Maruyama S, Yamakawa A, Nakamura E. ^{53}Mn–^{53}Cr chronometry of CB chondrite: Evidence for uniform distribution of 53mn in the early solar system. The Astrophysical Journal. 2010; 723:20–24.

Yasui C, Kobayashi N, Tokunaga AT, Saito M. Rapid evolution of the innermost dust disk of protoplanetary disks surrounding intermediate-mass stars. Monthly Notices of the Royal Astronomical Society. 2014; 442:2543–2559.

Yin, Z-Z.; Amelin, Y.; Jacobsen, B. Project milestones: Testing consistent chronologies between extinct 5^3Mn-5^3Cr and extant U-Pb systematics in the early solar system. 40th Lunar and Planetary Science Conference. CD-ROM; 2009. (abstract #2060)

Zartman, RE.; Jagoutz, E.; Bowring, SA. Pb-Pb Dating of the D'Orbigny and Asuka 881371 angrites and a second absolute time calibration of the Mn-Cr chronometer. 37th Lunar and Planetary Science Conference. CD-ROM; 2006. (abstract #1580)

Europe PMC Funders Author Manuscripts

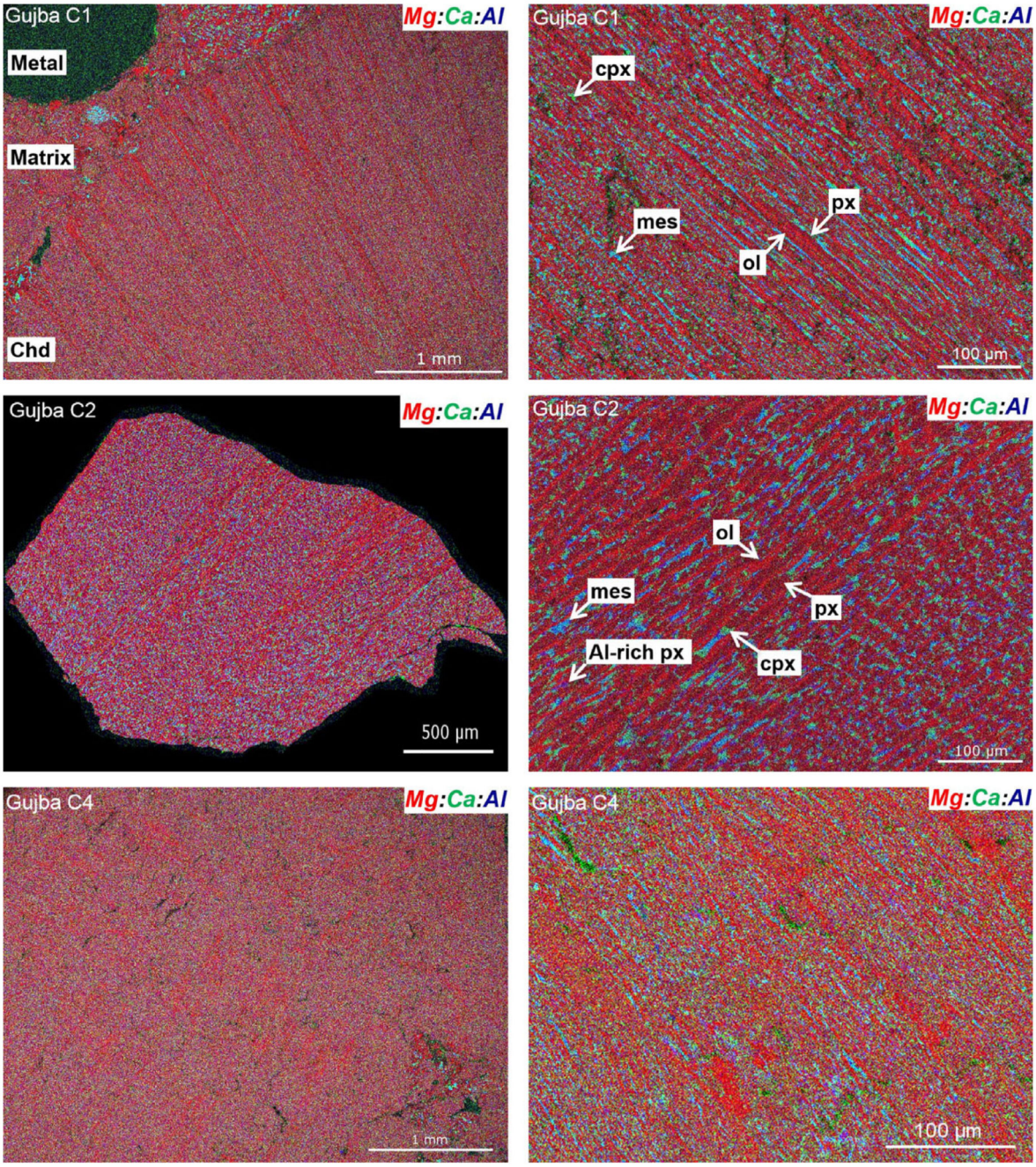

Fig. 1.

Combined X-ray elemental map of Gujba chondrule C1, C2, and C4. Colors represent Mg (red), Ca (green), and Al (blue). ol = olivine; px = sub-Ca pyroxene; cpx = high-Ca pyroxene; mes = mesostasis; Al-rich px = Al-rich low-Ca pyroxene. C1 has a radial pyroxene texture and C5 a barred olivine–pyroxene texture. Right-hand panels depict enlarged regions of chondrule textures shown on left-hand panels.

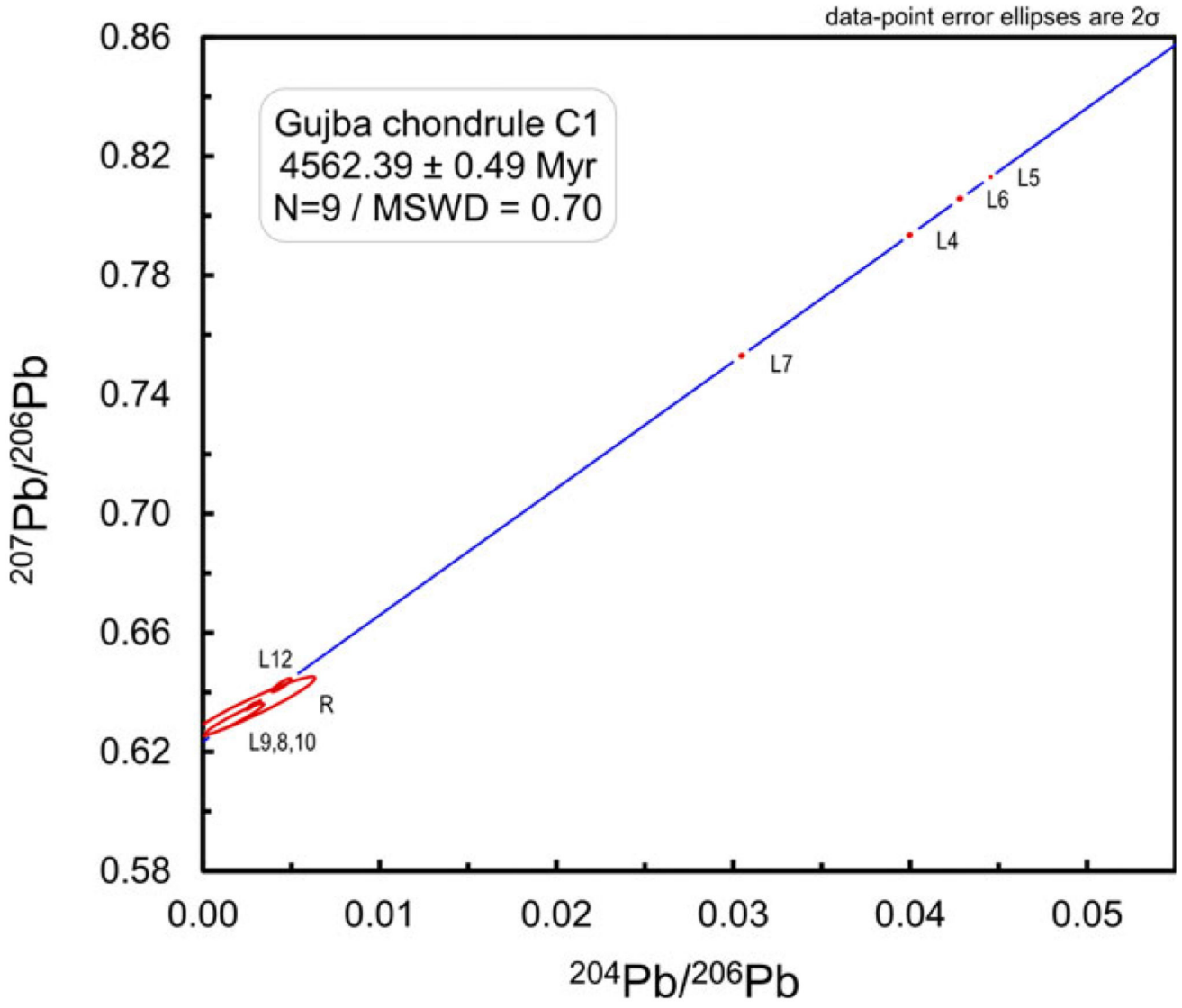

Fig. 2.

Pb-Pb isochron diagrams of Pb isotope analyses of Gujba chondrule C1. *N* = number of fractions. MSWD = mean square of weighted deviations. Regression parameters: slope = 4.2562 ± 0.0064, intercept = 0.62334 ± 0.00021 (uncertainties are 95% confidence intervals).

Europe PMC Funders Author Manuscripts

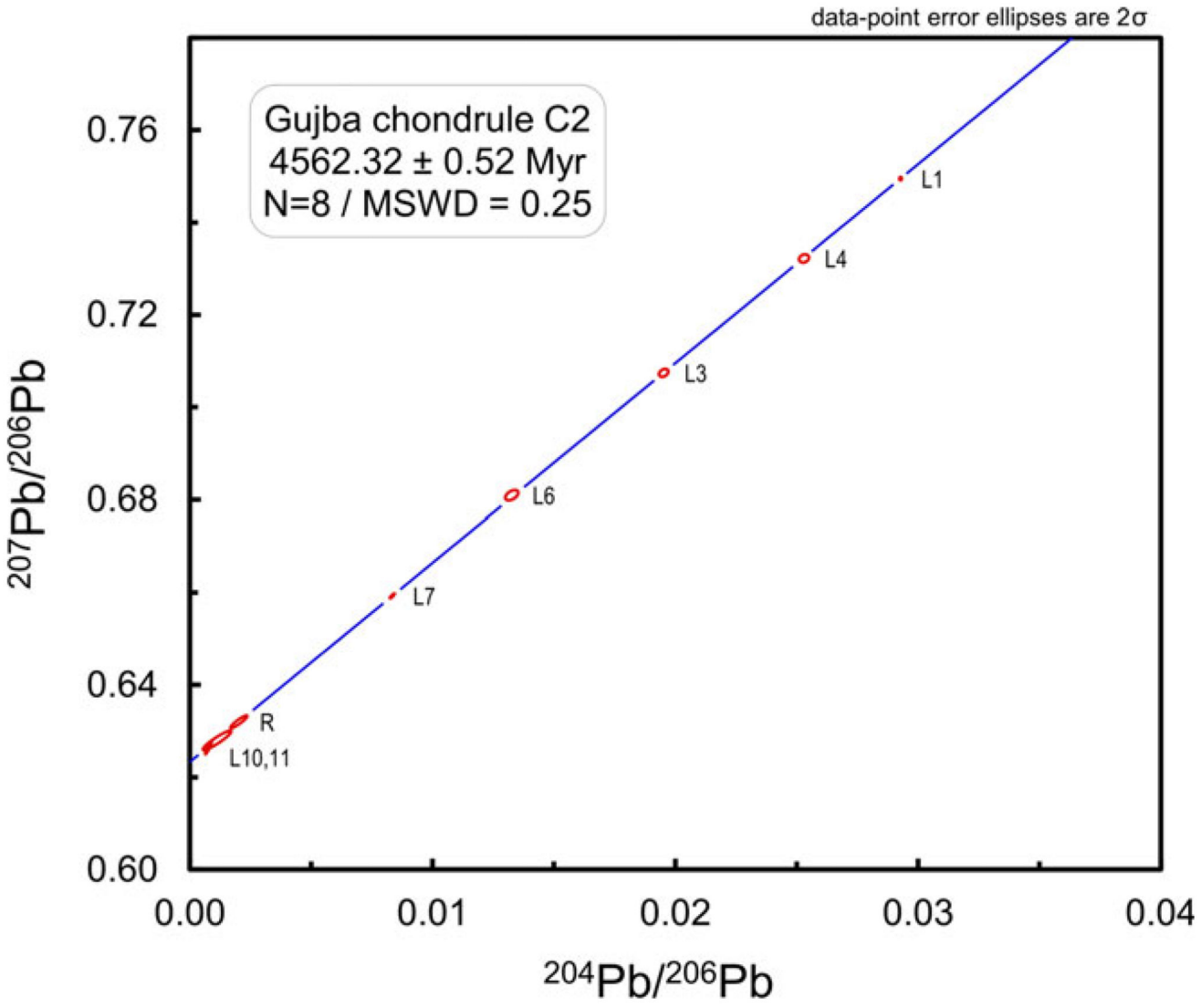

Fig. 3.

Pb-Pb isochron diagrams of Pb isotope analyses of Gujba chondrule C2. *N* = number of fractions. MSWD = mean square of weighted deviations. Regression parameters: slope = 4.3106 ± 0.015, intercept = 0.62331 ± 0.00022 (uncertainties are 95% confidence intervals).

Europe PMC Funders Author Manuscripts

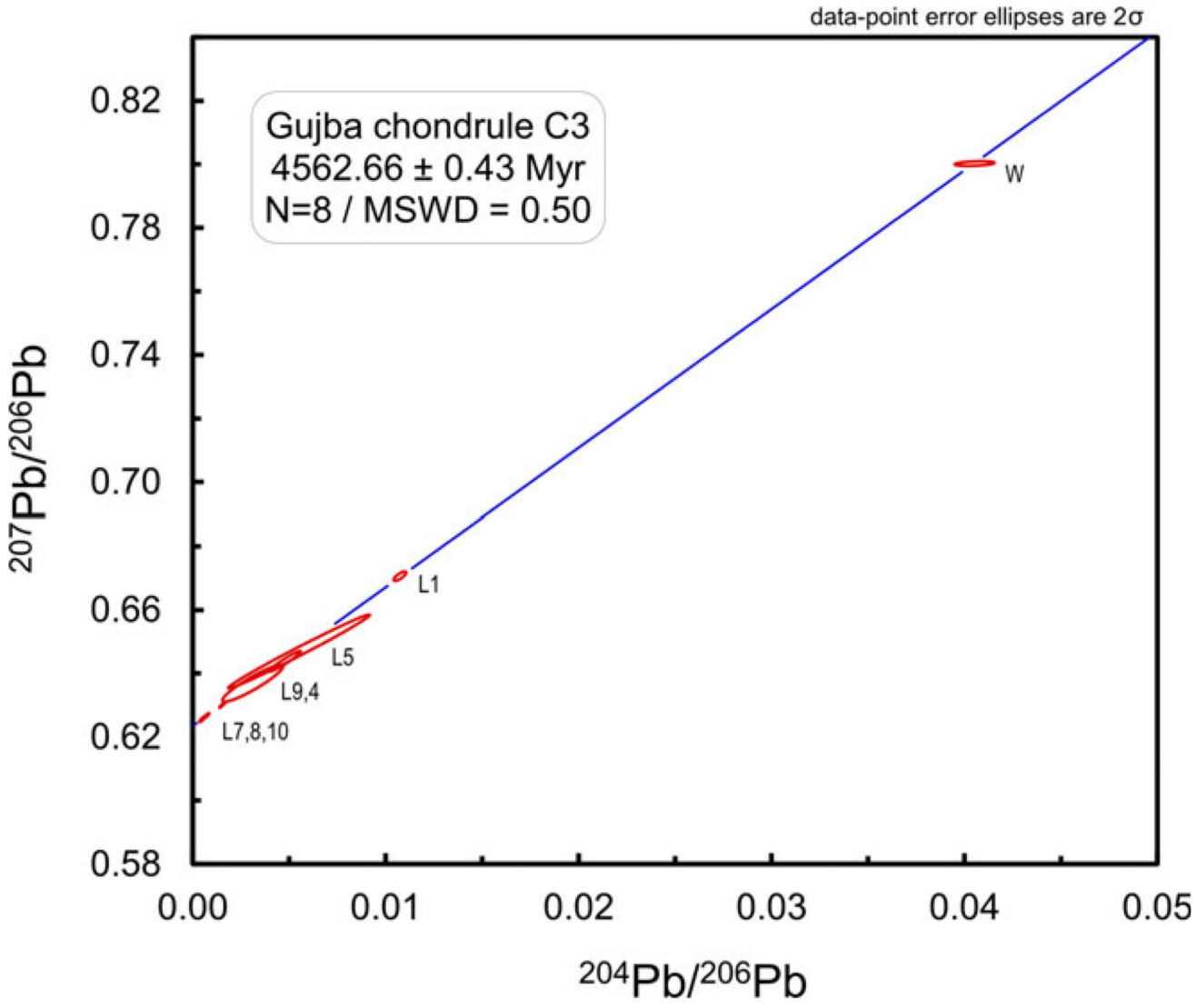

Fig. 4.

Pb-Pb isochron diagrams of Pb isotope analyses of Gujba chondrule C3. *N* = number of fractions. MSWD = mean square of weighted deviations. Regression parameters: slope = 4.366 ± 0.057, intercept = 0.62346 ± 0.00019 (uncertainties are 95% confidence intervals).

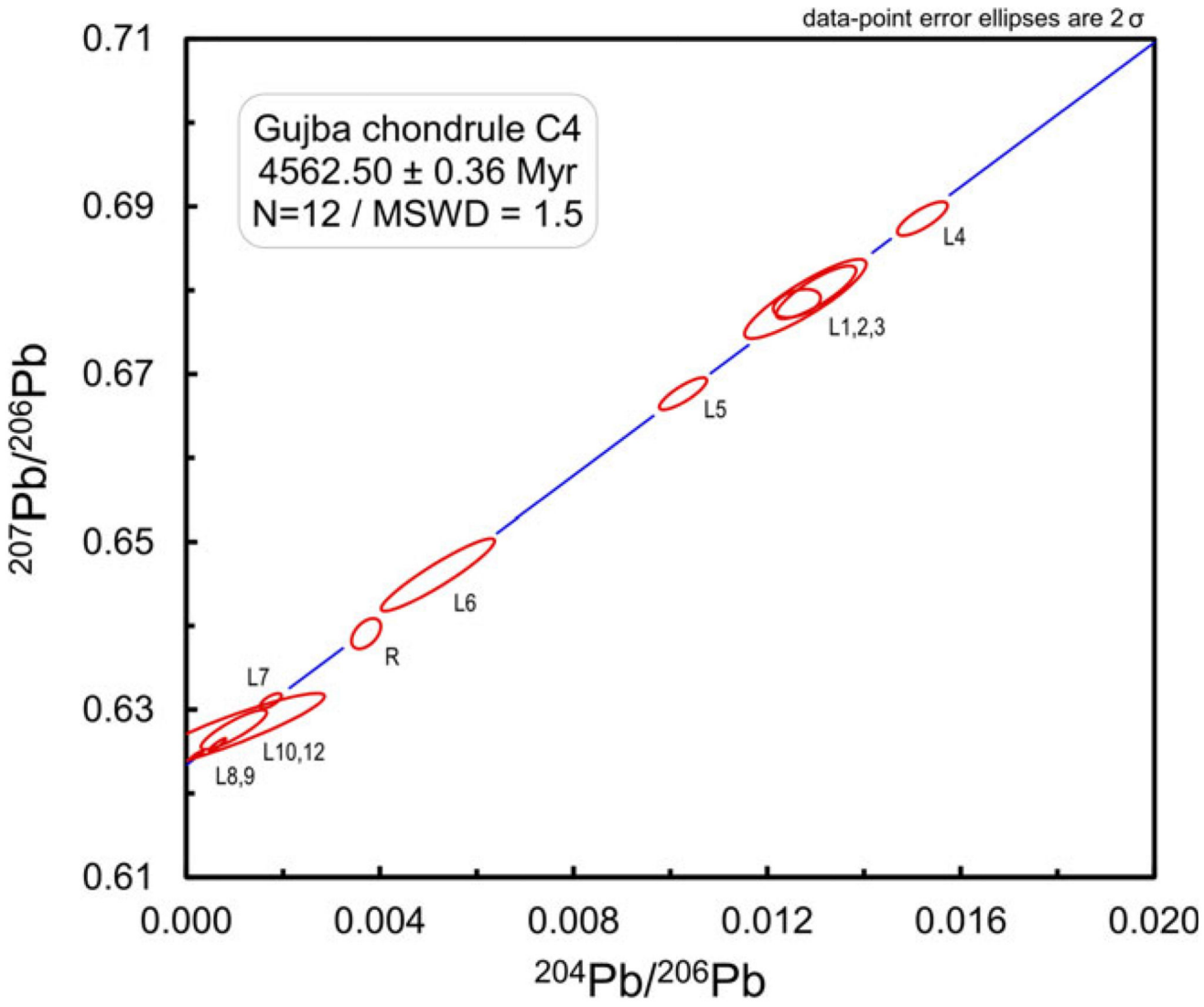

Fig. 5.

Pb-Pb isochron diagrams of Pb isotope analyses of Gujba chondrule C4. *N* = number of fractions. MSWD = mean square of weighted deviations. Regression parameters: slope = 4.309 ± 0.049, intercept = 0.62339 ± 0.00016 (uncertainties are 95% confidence intervals).

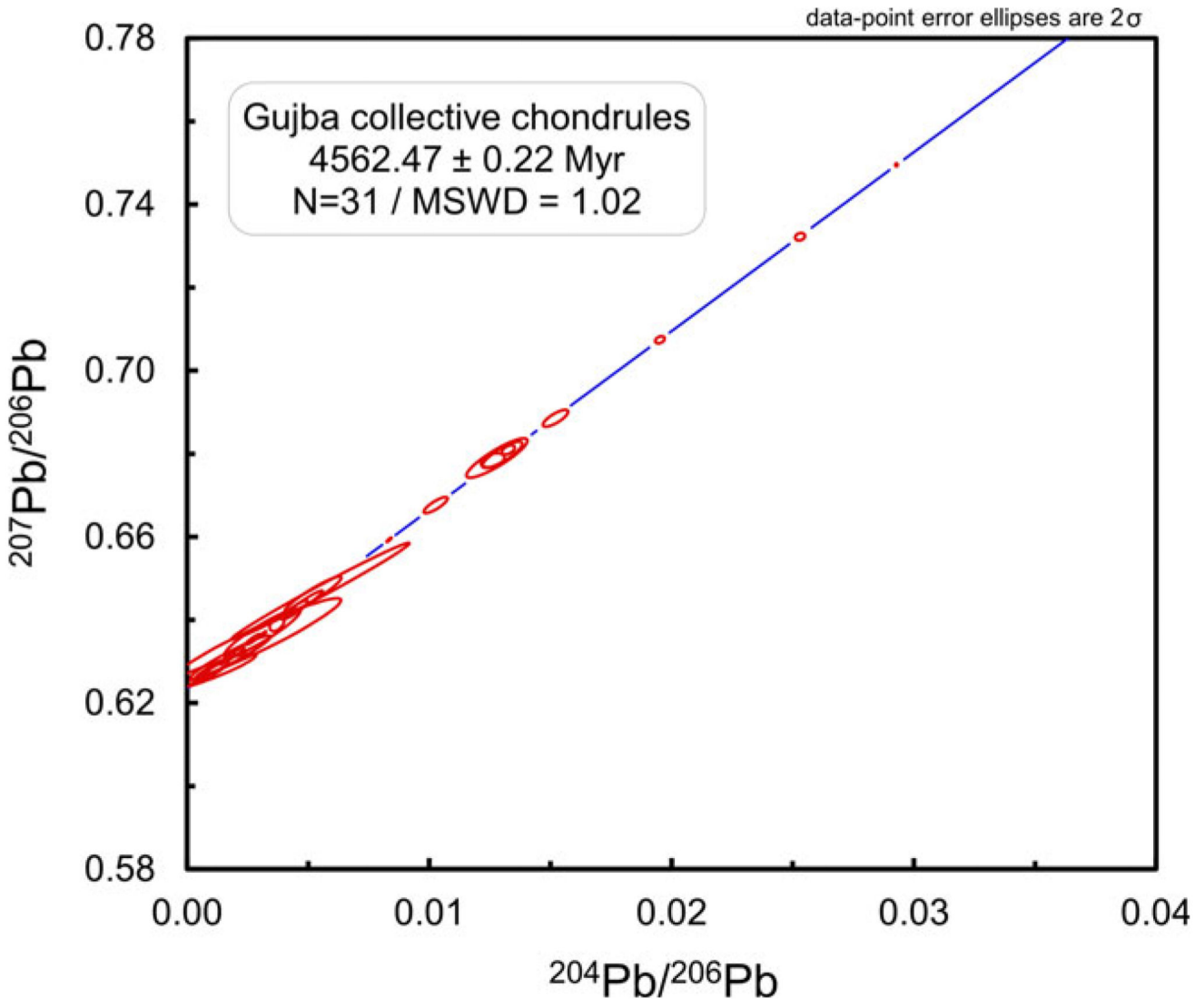

Fig. 6.

Pb-Pb isochron diagrams of Pb isotope analyses of all four Gujba chondrules (C1, C2, C3, and C4). *N* = number of fractions. MSWD = mean square of weighted deviations. Regression parameters: slope = 4.3062 ± 0.011, intercept = 0.623380 ± 0.000094 (uncertainties are 95% confidence intervals).

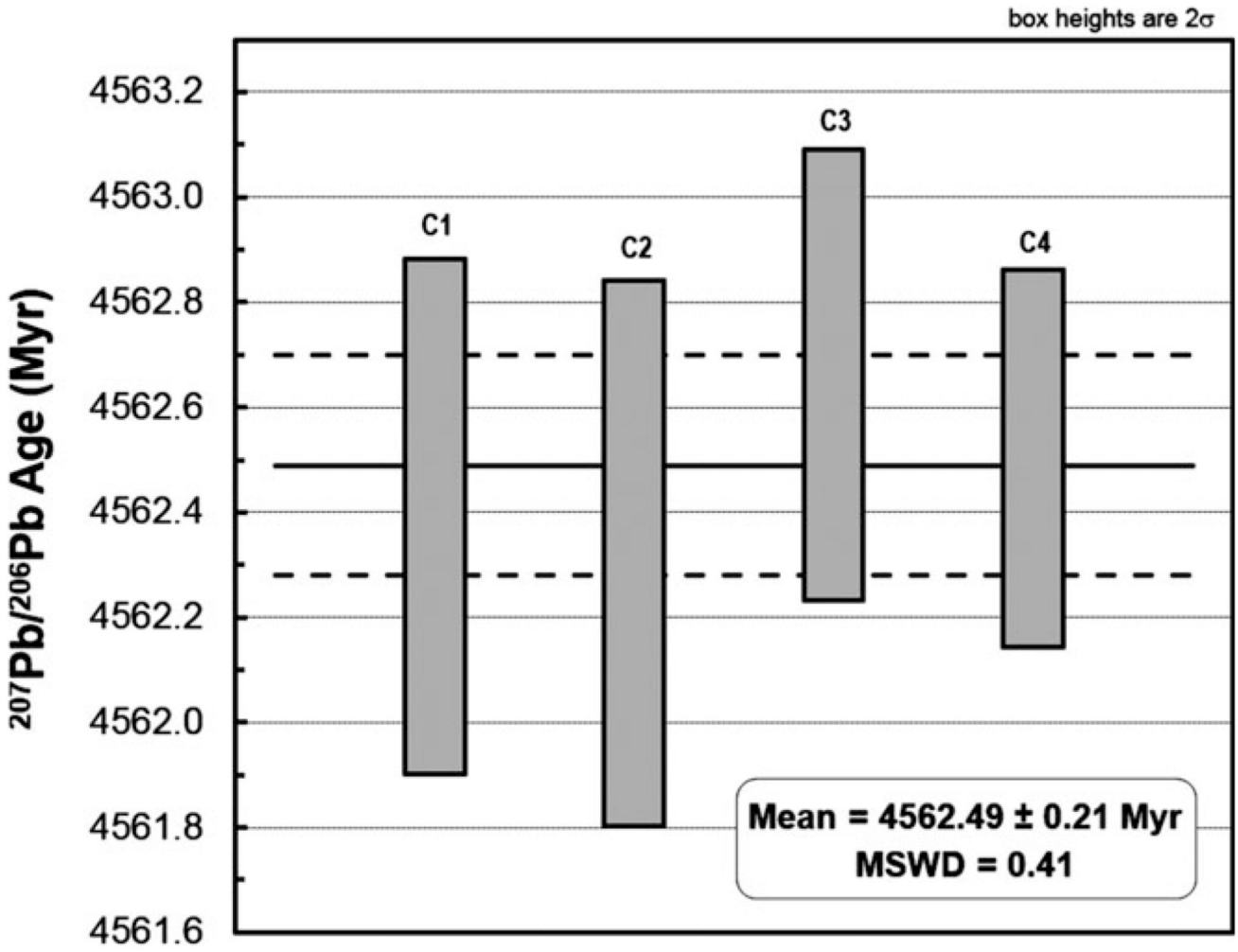

Fig. 7.
$^{207}Pb^*/^{206}Pb^*$ ages for four Gujba chondrules, and the associated weighted average.

Europe PMC Funders Author Manuscripts

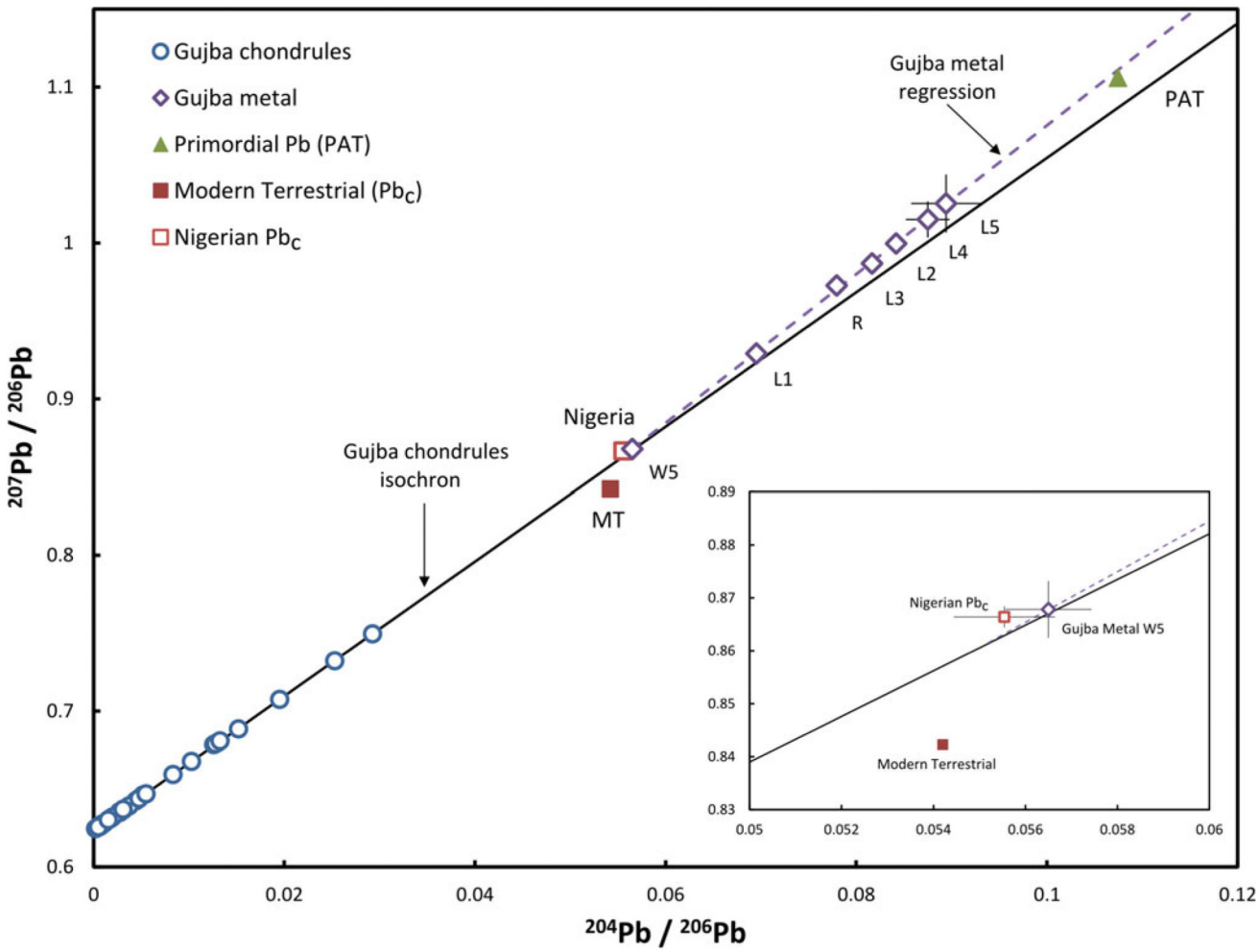

Fig. 8.

$^{204}Pb/^{206}Pb$ versus $^{207}Pb/^{206}Pb$ diagram for Gujba chondrules and metal digestion steps. MT (dark square) = average modern terrestrial Pb (Stacey and Kramers 1975), PAT (triangle) = primordial Pb (defined by Tatsumoto et al. 1973), Nigeria (light square) = local Nigerian terrestrial contaminant Pb (Smith et al. 1996). Gujba chondrules dissolution steps (circles) define an isochron representative of a binary mixture of radiogenic Pb (Pb_r) and terrestrial contaminant Pb (Pb_c). Gujba metal dissolution steps (diamonds) regress in a line representative of a binary mixture of Pb_c and primordial Pb (Pb_i). Inset showing expanded Pb-Pb diagram of approximation of terrestrial contaminant Pb.

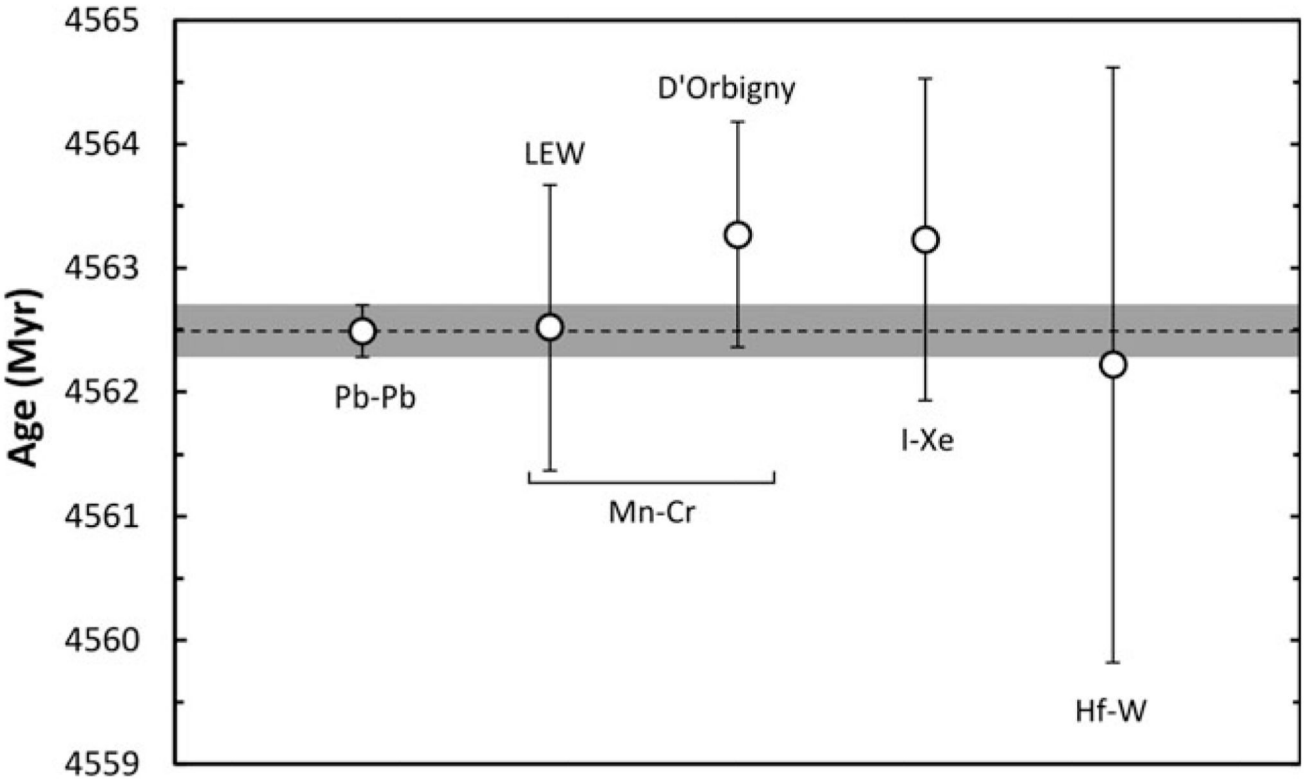

Fig. 9.

Comparison of absolute Pb-Pb Gujba age with different short-lived radionuclide chronometers. Data sources are as follow: Pb-Pb, this study; Mn-Cr, Yamashita et al. (2010) relative to data of Lugmair and Shukolyukov (1998) for LEW 86010 and relative to data of Glavin et al. (2004) for D'Orbigny; I-Xe, Gilmour et al. (2009), relative to Shallowater Brazzle et al. (1999); Hf-W, Kleine et al. (2005) relative to Kleine et al. (2004) and Kruijer et al. (2014b). The reference Pb-Pb ages for the short-lived radionuclide chronometers are mentioned in the text. Error bars (2σ) are calculated to include the errors on the isochron slopes for Gujba and the reference meteorite and the uncertainty of the reference meteorite Pb-Pb age.

Europe PMC Funders Author Manuscripts

Europe PMC Funders Author Manuscripts

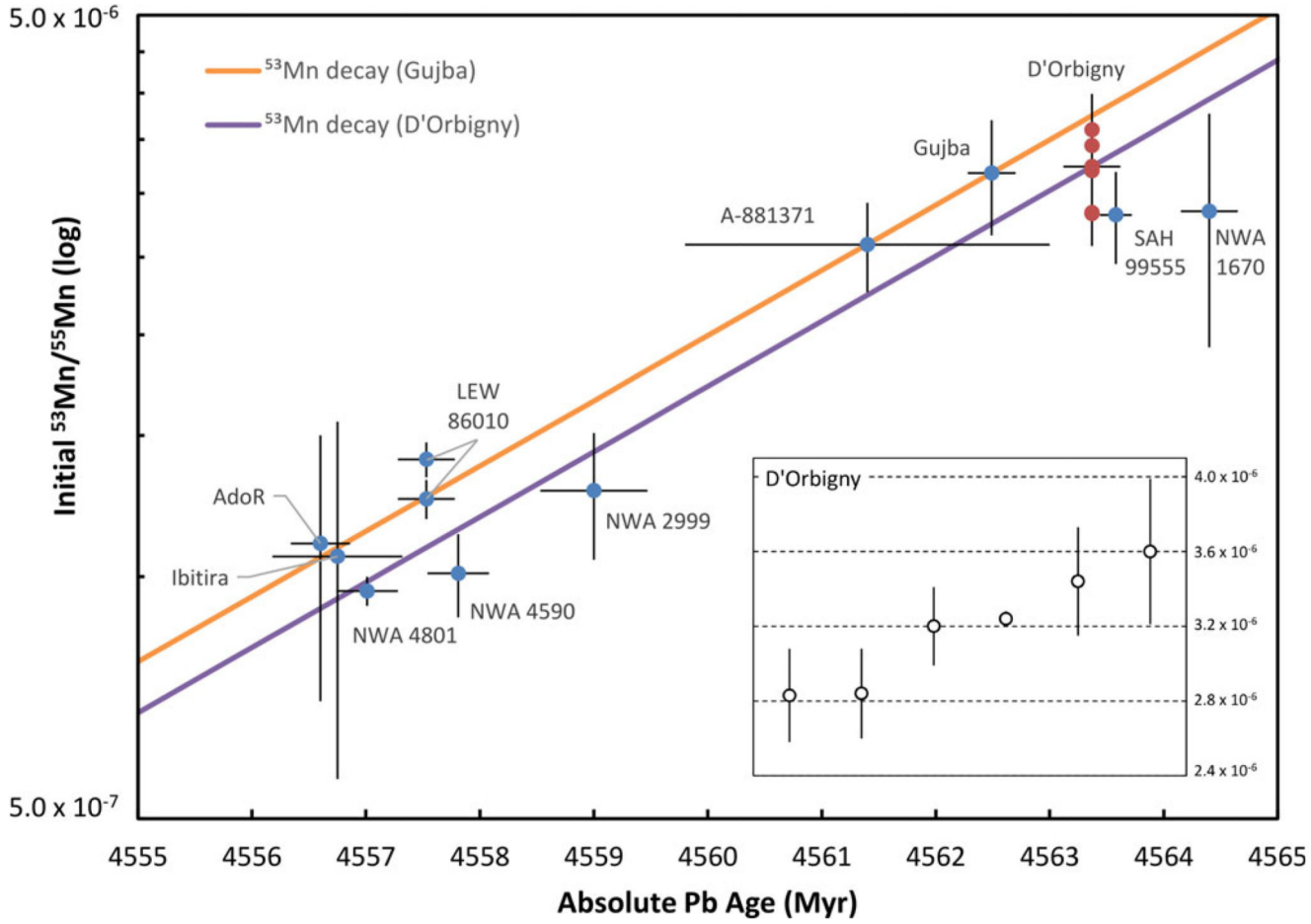

Fig. 10.

Pb-Pb ages versus initial $^{53}Mn/^{55}Mn$ for angrite, eucrite, and CB meteorites. Pb-Pb ages are from: Brennecka and Wadhwa (2012) for D'Orbigny, Angra dos Reis (hereafter "AdoR") NWA 4801 and NWA 4590; Iizuka et al. (2014) for LEW 86010 and Ibitira; Connelly et al. (2008) U-corrected for Sahara 99555 (hereafter "SAH 99555") and Connelly (personal communication) for NWA 1670 and NWA 2999; Zartman et al. (2006) U-corrected for Asuka 881371 (hereafter "A-881371"); this study for Gujba. Initial $^{53}Mn/^{55}Mn$ values are from: Glavin et al. (2004) for D'Orbigny, Sugiura et al. (2005) for Sahara, Asuka, and NWA 1670; Lugmair and Shukolyukov (1998) and Nyquist et al. (1994) for LEW and Ibitira; McKibbin et al. (2013) for AdoR; Shukolyukov et al. (2009) for NWA 4801; Shukolyukov and Lugmair (2008) for NWA 2999; Yin et al. (2009) for NWA 4590; Yamashita et al. (2010) for Gujba. Other values for D'Orbigny are from Nyquist et al. (2003), Sugiura et al. (2005), Yin et al. (2009) and McKibbin et al. (2013) as shown in the inserted plot. The two ^{53}Mn decay lines are anchored to the initial $^{53}Mn/^{55}Mn$ for Gujba given by Yamashita et al. (2010) and for D'Orbigny given by Glavin et al. (2004).

Europe PMC Funders Author Manuscripts

Table 1

Summary of ages for Gujba chondrite using different chronometers.

Method	Materials	Initial	Anchor	Age U-corrected[e]	Reference
U-Pb	Chondrule	–	–	4561.68 ± 0.51	*1*
Mn-Cr	Chondrule/metal	$^{53}Mn/^{55}Mn$ $(3.18 \pm 0.52) \times 10^{-6}$	D'Orbigny[a] $(3.24 \pm 0.04) \times 10^{-6}$ 4563.37 ± 0.25	4563.3 ± 0.9	*2*
			LEW86010[b] $(1.25 \pm 0.07) \times 10^{-6}$ 4557.53 ± 0.25	4562.5 ± 1.1	
I-Xe	Chondrule	$^{129}I/^{127}I$ $(1.16 \pm 0.02) \times 10^{-4}$	Shallowater[c] $(1.072 \pm 0.02) \times 10^{-4}$ 4562.3 ± 0.8	4563.2 ± 1.3	*3*
Hf-W	Metal	$\varepsilon^{182}W$ −2.97 ± 0.16	CAI[d] 4567.30 ± 0.16	4562.2 ± 2.4	*4*

[a] Glavin et al. (2004); Brennecka and Wadhwa (2012).

[b] Lugmair and Shukolyukov (1998); Amelin (2008).

[c] Brazzle et al. (1999); Gilmour et al. (2009).

[d] Connelly et al. (2012).

[e] Corrected using $^{238}U/^{235}U = 137.786 \pm 0.013$.

References: (1) Krot et al. (2005); (2) Yamashita et al. (2010); (3) Gilmour et al. (2009); (4) Kleine et al. (2005).

Europe PMC Funders Author Manuscripts

Table 2

Pb isotope analyses of the SRM-982 reference standard during the course of this study.

SRM-982 standard	$^{206}Pb/^{204}Pb$	2SE	$^{207}Pb/^{206}Pb$	2SE
1	36.745742	0.014573	0.467062	0.000074
2	36.721561	0.027837	0.467072	0.000145
3	36.724861	0.022760	0.467100	0.000117
4	36.752794	0.015318	0.467155	0.000074
5	36.729906	0.025568	0.467186	0.000157
6	36.727710	0.011665	0.467072	0.000054
7	36.758083	0.022255	0.467039	0.000110
8	36.752202	0.010585	0.467120	0.000054
9	36.725293	0.015354	0.467089	0.000086
10	36.748559	0.020989	0.467075	0.000115
11	36.711980	0.010121	0.467020	0.000050
12	36.726637	0.013612	0.467179	0.000065
13	36.747877	0.017168	0.467042	0.000142
14	36.720595	0.016461	0.467102	0.000084
15	36.725182	0.012111	0.467197	0.000058
16	36.732675	0.011150	0.467195	0.000055
17	36.749615	0.013241	0.467094	0.000053
18	36.758620	0.015373	0.467011	0.000100
19	36.719447	0.017488	0.467077	0.000085
20	36.730312	0.024187	0.467072	0.000127
21	36.730203	0.027625	0.467317	0.000162
22	36.723632	0.014433	0.467025	0.000086
23	36.713073	0.020829	0.467102	0.000120
24	36.771984	0.028911	0.467271	0.000137
25	36.697760	0.015288	0.467262	0.000090
26	36.723179	0.021310	0.467184	0.000090
27	36.745221	0.020319	0.467136	0.000142
28	36.741355	0.013525	0.467080	0.000082
29	36.758790	0.013946	0.467078	0.000073
30	36.706886	0.018546	0.467178	0.000090
31	36.711900	0.018373	0.467112	0.000090
32	36.777560	0.033488	0.467057	0.000151
33	36.725587	0.010635	0.467052	0.000069
34	36.758454	0.018590	0.467080	0.000111
Average	*36.735154*		*0.467114*	
2SD	*0.0381753*		*0.0001490*	
Reproducibility (%)	*0.104*		*0.032*	

All data acquired by sequentially peak jumping the ion beams into the central SEM-ion counting system. Mass fractionation correction using the $^{208}Pb/^{206}Pb$ value and linear law.

Europe PMC Funders Author Manuscripts

Europe PMC Funders Author Manuscripts

Table 3

Pb isotope data for Gujba chondrules and metal.

Sample	Acid	Treatment	Duration[a]	Pb (pg)	$^{206}Pb/^{204}Pb$ (raw)	$^{204}Pb/^{206}Pb$	2SE(%)	$^{207}Pb/^{206}Pb$	2SE(%)	Rho[b]
Gujba chondrule C1 (123.7 mg)										
L1	1M HBr	US/HP(110°)/US	5/15/5	172.6	22.99	0.043284	0.48	0.804549	0.11	0.01
L2	2M HCl	US/HP/US	5/5/5	not analyzed						
L3	3M HNO_3	US/HP/US	5/5/5	155.2	27.01	0.036804	0.54	0.779517	0.11	0.22
L4*	4M HNO_3	US/HP/US	5/10/5	296.6	24.90	0.039976	0.21	0.793531	0.05	0.15
L5*	2M HCl	US/HP/US	5/45/5	936.4	22.37	0.044563	0.05	0.812981	0.02	0.02
L6*	6M HCl	US/HP/US	5/5/5	204.2	23.24	0.042813	0.22	0.805733	0.05	0.16
L7*	6M HCl	US/HP/US	5/45/5	524.3	32.66	0.030470	0.25	0.753047	0.06	0.16
L8*	1M HF	US/HP/US	5/5/5	821.2	312.86	0.003152	2.92	0.636627	0.08	0.90
L9*	1M HF	US/HP/US	5/30/5	74.4	457.64	0.001796	75.42	0.631000	0.68	0.96
L10*	7M HF	US/HP/US	5/20/5	37.3	282.83	0.002780	104.99	0.634891	1.33	0.95
L11	7M HF	US/HP/US	5/30/5	9.5	180.56	0.002706	1338.37	0.635121	5.40	0.99
L12*	28M HF-14M HNO_3	US/HP/US	5/35/5	172.6	216.80	0.004434	10.17	0.642373	0.29	0.90
Residue	28M HF-14M HNO_3	HP(130°)	48 h	316.5	353.44	0.002730	9.12	0.635330	0.17	0.92
Gujba chondrule C2 (91.8 mg)										
L1*	1M HBr	US/HP(110°)/US	5/15/5	306.5	34.01	0.029277	0.13	0.749502	0.04	0.03
L2	2M HCl	US/HP/US	5/5/5	236.6	34.07	0.029196	0.14	0.749622	0.04	0.08
L3*	3M HNO_3	US/HP/US	5/5/5	87.0	50.65	0.019520	0.80	0.707417	0.10	0.33
L4*	4M HNO_3	US/HP/US	5/10/5	69.4	39.19	0.025301	0.65	0.732209	0.10	0.21
L5	2M HCl	US/HP/US	5/45/5	165.6	50.01	0.019848	0.42	0.709308	0.06	0.14
L6*	6M HCl	US/HP/US	5/55/5	74.6	74.15	0.013263	1.63	0.680927	0.13	0.48
L7*	6M HCl	US/HP/US	5/45/5	219.5	118.55	0.008340	0.97	0.659284	0.06	0.91
L8	1M HF	US/HP/US	5/5/5	937.2	3793.92	0.000246	8.95	0.625183	0.03	0.15
L9	1M HF 7M	US/HP/US	5/30/5	not analyzed						
L10*	HF	US/HP/US	5/20/5	192.9	1172.49	0.000770	14.19	0.626443	0.19	0.92
L11*	7M HF	US/HP/US	5/30/5	48.8	694.56	0.001125	42.35	0.627994	0.27	0.93
L12	28M HF-14M	US/HP/US	5/30/5 48 h	not analyzed						
Residue*	HNO_3 28M HF-14M HNO_3	HP(130°)	48 h	73.4	447.44	0.002022	13.92	0.632020	0.18	0.92
Gujba chondrule C3										
W1-9*	Eth-Ace-H_2O	N/A	N/A	124.0	24.40	0.040528	2.07	0.800227	0.07	0.34
L1*	2M HBr	N/A	N/A	160.6	88.76	0.010740	2.43	0.670627	0.18	0.77
L2	2M HCl	N/A	N/A	12.1	44.73	0.019363	16.51	0.706436	1.63	0.99
L3	H2O	N/A	N/A	68.0	40.87	0.005001	13.33	0.640873	0.41	0.99
L4*	4M HNO_3	N/A	N/A	68.1	165.50	0.004783	13.96	0.643821	0.41	0.96
L5*	2M HCl	N/A	N/A	18.3	103.19	0.005506	54.47	0.646915	1.47	0.99

Sample	Acid	Treatment	Duration[a]	Pb (pg)	$^{206}Pb/^{204}Pb$ (raw)	$^{204}Pb/^{206}Pb$	2SE(%)	$^{207}Pb/^{206}Pb$	2SE(%)	Rho[b]
L6	6M HCl	N/A	N/A	60.6	66.12	0.013902	4.65	0.688617	0.37	0.95
L7*	1M HF	N/A	N/A	396.5	1070.14	0.000703	17.27	0.626642	0.11	0.92
L8*	1M HF	N/A	N/A	421.4	1400.21	0.000494	24.07	0.625614	0.12	0.89
L9*	6M HCl	N/A	N/A	41.3	191.96	0.003110	41.36	0.636903	0.74	0.92
L10*	28M HF-14M HNO_3	N/A	N/A	355.0	555.90	0.001540	8.41	0.630132	0.12	0.95
Gujba chondrule C4 (43.1 mg)										
L1*	1M HBr	US/HP(110°)/US	5/5/5	43.6	77.14	0.012615	3.17	0.678423	0.20	0.39
L2*	2M HCl	US/HP/US	5/5/5	23.7	73.46	0.013013	5.18	0.679736	0.38	0.84
L3*	3M HNO_3	US/HP/US	5/5/5	15.8	73.15	0.012790	8.04	0.678955	0.57	0.88
L4*	4M HNO_3	US/HP/US	5/20/5	35.5	64.00	0.015208	2.78	0.688535	0.24	0.78
L5*	2M HCl	US/HP/US	5/45/5	42.1	94.15	0.010263	3.90	0.667634	0.24	0.83
L6*	6M HCl	US/HP/US	5/5/5	20.4	169.13	0.005198	18.44	0.646100	0.55	0.94
L7*	6M HCl	US/HP/US	5/60/5	109.5	530.83	0.001744	10.42	0.631045	0.12	0.70
L8*	1M HF	US/HP/US	5/5/5	211.9	3477.06	0.000217	50.18	0.624556	0.07	0.90
L9*	1M HF	US/HP/US	5/15/5	147.7	1340.34	0.000645	21.87	0.625817	0.10	0.92
L10*	7M HF	US/HP/US	5/20/5	20.9	626.60	0.000894	179.67	0.627417	0.59	0.92
L11	7M HF	US/HP/US	5/20/5	8.7	324.79	0.001427	459.68	0.629433	1.41	0.91
L12*	28M HF-14M HNO_3	US/HP/US	5/30/5	42.3	751.45	0.000983	56.53	0.627605	0.31	0.87
Residue*	28M HF-14M HNO_3	HP(130°)	24 h	76.2	255.14	0.003715	6.65	0.639077	0.23	0.48
Gujba metal (86.3 mg)										
W5	H20	HP(120°)	24 h	7.74	17.51	0.056500	1.65	0.867823	0.62	
L1	0.5M HBr	HP/US	90/5	49.79	14.36	0.069536	0.48	0.928997	0.19	
L2	0.5M HBr	HP/US	90/5	34.84	11.88	0.084182	1.06	0.999697	0.43	
L3	1M HBr	HP/US	60/5	23.94	12.25	0.081650	1.41	0.986839	0.58	
L4	2M HCl	HP/US	30/5	14.45	11.46	0.087499	2.63	1.015070	1.13	
L5	6M HCl	HP/US	30/5	9.59	11.27	0.089425	4.11	1.025297	1.81	
Residue	6M HCl	HP(130°)	48 h	24.84	12.81	0.077946	1.25	0.972664	0.51	

All fractions subjected to a precleaning routine of five cycles of ethanol, acetone, and water on the hotplate and ultrasonic followed by six steps of 0.02M HBr on the hotplate and ultrasonic bath.

The $^{206}Pb/^{204}Pb$ reflects the raw $^{206}Pb/^{204}Pb$ ratio and is not corrected for mass fractionation, blank contribution, and spike addition. All other ratios are corrected for mass fractionation (using the $^{205}Pb/^{202}Pb$), blank contribution, and spike addition, and these corrections are propagated in the quoted uncertainties.

[a]Time in minutes unless indicated as hours by “h.”

*Fractions included in regression calculations.

[b]The Rho value is the error correlation between $^{204}Pb/^{206}Pb$ and $^{207}Pb/^{206}Pb$ ratios.

US = ultrasonic bath; HP = hotplate.

Europe PMC Funders Author Manuscripts

Table 4

Summary of four Gujba chondrules analyzed with regressed absolute Pb-Pb ages.

Chondrule	Weight (mg)	Pb_r (ng)	Pb_r (ppb)	Age (Myr)	MSWD	*N*
C1	123.7	3.8	30.7	4562.39 ± 0.49	0.70	9
C2	91.8	2.5	27.2	4562.32 ± 0.52	0.25	8
C3	–	1.6	–	4562.66 ± 0.43	0.50	8
C4	43.1	0.8	18.6	4562.50 ± 0.36	1.50	12
Collective	–	–	–	4562.47 ± 0.22	1.02	31
Mean	–	–	–	*4562.49 ± 0.21*	0.41	4

MSWD = mean square of weighted deviations; *N* = number of fractions used in the regression.

Europe PMC Funders Author Manuscripts

Table 5

Summary of ages for Gujba chondrite using different chronometers and subsequent offset compared to absolute Pb-Pb chronometer.

Chronometer	Pb-Pb	Mn-Cr	I-Xe	Hf-W
Age (Myr) of Gujba	4562.49 ± 0.21 (this study)	4562.52 ± 1.15[a] 4563.27 ± 0.91[b]	4563.23 ± 1.30	4562.2 ± 2.4
Offset (Myr)	–	−0.03 ± 1.16[a] −0.78 ± 0.93[b]	0.74 ± 1.32	−0.3 ± 2.4

[a] LEW 86010 anchored age.

[b] D'Orbigny anchored age.